remote sensing

MDPI

Article

Riparian Plant Evapotranspiration and Consumptive Use for Selected Areas of the Little Colorado River Watershed on the Navajo Nation

Pamela L. Nagler [1,*], Armando Barreto-Muñoz [2], Ibrahima Sall [3], Matthew R. Lurtz [4] and Kamel Didan [2]

1 U.S. Geological Survey, Southwest Biological Science Center, Tucson, AZ 85719, USA
2 Biosystems Engineering, University of Arizona, Tucson, AZ 85721, USA
3 Agricultural and Resource Economics, University of Arizona, Tucson, AZ 85721, USA
4 Civil and Environmental Engineering, Colorado State University, Fort Collins, CO 80523, USA
* Correspondence: pnagler@usgs.gov; Tel.: +1-520-670-3357

Abstract: Estimates of riparian vegetation water use are important for hydromorphological assessment, partitioning within human and natural environments, and informing environmental policy decisions. The objectives of this study were to calculate the actual evapotranspiration (ETa) (mm/day and mm/year) and derive riparian vegetation annual consumptive use (CU) in acre-feet (AF) for select riparian areas of the Little Colorado River watershed within the Navajo Nation, in northeastern Arizona, USA. This was accomplished by first estimating the riparian land cover area for trees and shrubs using a 2019 summer scene from National Agricultural Imagery Program (NAIP) (1 m resolution), and then fusing the riparian delineation with Landsat-8 OLI (30-m) to estimate ETa for 2014–2020. We used indirect remote sensing methods based on gridded weather data, Daymet (1 km) and PRISM (4 km), and Landsat measurements of vegetation activity using the two-band Enhanced Vegetation Index (EVI2). Estimates of potential ET were calculated using Blaney-Criddle. Riparian ETa was quantified using the Nagler ET(EVI2) approach. Using both vector and raster estimates of tree, shrub, and total riparian area, we produced the first CU measurements for this region. Our best estimate of annual CU is 36,983 AF with a range between 31,648–41,585 AF and refines earlier projections of 25,387–46,397 AF.

Keywords: evapotranspiration; EVI2; riparian ecosystem; water requirement; consumptive use; Daymet; PRISM; Blaney-Criddle

check for updates

Citation: Nagler, P.L.; Barreto-Muñoz, A.; Sall, I.; Lurtz, M.R.; Didan, K. Riparian Plant Evapotranspiration and Consumptive Use for Selected Areas of the Little Colorado River Watershed on the Navajo Nation. *Remote Sens.* **2023**, *15*, 52. https://doi.org/10.3390/rs15010052

Academic Editors: Miloš Rusnák, Monika Šulc Michalková, Anna Kidová, Zdeněk Máčka, László Bertalan, Maciej Liro and Malia A. Volke

Received: 23 November 2022
Revised: 13 December 2022
Accepted: 20 December 2022
Published: 22 December 2022

1. Introduction

Accurate estimates of riparian water use by actual evapotranspiration (ETa, mm/day and mm/year) are important to quantify so that in-stream use can be partitioned for human and natural environments. Natural grasses, shrubs, and trees that grow alongside rivers and streams are collectively called riparian vegetation and their leaves transpire water that is considered a loss to the ecosystem. Bare soil loses water through evaporation. We quantify both evaporation and transpiration losses in the landscape as one variable, evapotranspiration (ETa). The Terms section explains remote sensing of ETa. ETa is among one of the more difficult components of the water cycle to measure. Another is groundwater recharge; however, ETa encompasses interactions between plants and soil, the aquifer, and the atmosphere. Such feedbacks are well established, particularly between groundwater depth, energy flux, and runoff, but their measurements are difficult to accurately quantify, and thus they remain debatable. Actual evapotranspiration of riparian areas is a difficult component of the water cycle to quantify because it involves interactions with climate, vadose zone water, and exchanges between aquifers and surface water. Additionally, riparian ETa is less understood than agricultural ETa given that agriculture is directly connected to the food-energy-water nexus. In the southwestern US, riparian areas are estimated to be less than 2% of the total land area [1], yet these ecosystems contain a larger and more diverse number of species, are more productive, and serve more ecological functions compared to adjacent terrestrial uplands and other ecosystems in the desert [2]. Arid riparian areas are dynamic and disturbance-driven, leading to rapid changes in vegetation composition and environmental conditions [3,4]. For this reason, we utilize remote sensing methods that can capture the time series of vegetation greenness, phenology, and plant water use [5]. Most studies of remotely sensed ETa in uncultivated, riparian ecosystems were conducted in arid or semi-arid climates and used a myriad of validated methods [6,7]. Due to the relative fraction of land cover and its larger percentage of water use, agricultural lands have remained the focus of scientific studies that aim to quantify ETa. Therefore, accurately measuring water-use of uncultivated plants in the riparian zone, or riparian ETa, has rarely been included in water budgets because more accessible agricultural estimates have been used instead, i.e., crop coefficients; thermal agricultural-centered methods [6,7]. Due to clouds, haze, and confounding atmospheric conditions that are more prevalent in mesic climates, we know of very few remotely sensed time-series studies of ETa involving riparian corridors [7]. The literature available on studies of ETa that are not focused on arid/semi-arid riparian lands is somewhat limited, with some that utilize remote sensing methods [8]; yet studies that exist for non-arid riparian lands have contributed profound knowledge to what is known about the changes in these systems [9–12].

In this arid land study, we quantify ETa from riparian vegetation, both as a component of the water cycle and as a useful measure of groundwater discharge by vegetation. Groundwater levels may drop off at some distance from ephemeral channels, and as such, it is expected that vegetation increase dependency on soil-moisture over groundwater for ETa; however, for this study, we consider soil-moisture to be negligible. We wish to accentuate that these riparian areas are poorly understood around the world, especially in dry climates. More importantly, riparian areas are not well studied compared to agricultural regions given the direct ties to food security [13]. Riparian areas are even less understood on tribal lands because they are not as extensively studied as public lands. Quantifying riparian health on the Navajo Nation will lead to a better understanding of the water resources required to sustain indigenous people and ecosystems which are under threat from over-allocation of water to irrigated farming. The Nation has prioritized preserving these riparian areas for cultural reasons, including preservation of biodiversity. Riparian areas are (1) rich in medicinal plants, (2) provide habitat for animals of significance, and (3) provide unique landscapes of cultural importance.

In recent years, drought has impacted the Colorado Plateau [14,15]. Water shortages are a major threat to riparian areas because they are hotspots of biodiversity that act as refuges to aquatic and terrestrial flora [16]. Water shortages also threaten springs and groundwater dependent species (GDEs) in the Colorado River Basin [17]. Quantification of available water for riparian corridors and GDEs of the Little Colorado River is of critical importance in a drying climate. For this study, we focus on riparian shrubs and trees that depend on baseflow, or groundwater that discharges directly into the river, and isolated springs that are disconnected from the main tributaries. Conserving these tributaries, streams, and springs are a high priority to the Navajo Nation.

ETa has been estimated in riparian zones, for example Gribovszki et al., 2008 [18] used diurnal groundwater fluctuations and is among the few studies of ETa in uncultivated ecosystems; these studies are a small fraction of ETa research published on agricultural ETa. ETa is considered one of the most elusive measurements in the water cycle because it is difficult to quantify [19]. For decades, agricultural methods (i.e., crop coefficients) were used to estimate riparian species and areas, but these methods over-estimate riparian water use [19]. These crop coefficients were established in 1998 based on the best evidence available at the time [20,21]. Subsequent measurements of riparian ETa, validated with ground measurements of water use from eddy-covariance and Bowen ratio [22,23] and sap flow [24,25], have produced lower estimates of riparian water use compared to that from crop-coefficient estimations that are annually reported by the U.S. Bureau of Reclamation's Lower Colorado River Accounting System (LCRAS) [26,27]. Using a compilation of previous vegetation mapping for change detection [28], measurement and scaling [22,29,30], the first accurate vegetation index-based (VI-based) riparian water use measurement methods were developed for the Lower Colorado River (LCR) [30,31]. Based on a mean annual flow of 1.8 × 10 m^3 (million cubic meters, mcm) in the river, LCR riparian vegetation consumed about 2.1% of the flow and the non-native shrub, saltcedar (*Tamarix* spp.) consumed 1.0% of the flow, much lower than earlier estimates of riparian ETa [30,31].

1.1. Terms

Land and water managers are interested in riparian ETa and net water requirements for particular landscapes. The net irrigation requirement is defined as the Potential Evapotranspiration (PET) minus precipitation (PP) plus soil moisture and is referred to as consumptive groundwater use. In this arid land study, the amount of water needed to support riparian plants comes from groundwater [32]. Consumptive groundwater use is quantified by subtracting PP from ETa, assuming no change in soil water storage. Thus, the net water requirement or water demand for a given area is measured by adding PP and soil moisture and then subtracting this value from ETa [32]. The term net water requirement is also referred to as the water demand or water deficit (WD, mm/year) and is ETa minus PP and soil moisture storage, which is negligible in deserts, and therefore considered to be zero in this dryland study [32]. To quantify consumptive use (CU), the water required to sustain the riparian plants (the WD) is multiplied by the landscape acreage [32]. We focus primarily on the riparian vegetation communities adjacent to the stream as well as springs in the study area. We multiplied the riparian corridor area by the WD to determine the average annual CU or total water requirement (mm/year), which is measured in acre-feet (AF) and is a commonly used unit of measurement in water resources. The water requirement, water demand or WD is both positive (when there is not enough water for plants) and negative (when there is enough water for plants).

Potential evapotranspiration (ETo) is measured from a reference surface that is a hypothetical grass that is one-foot tall and covers one acre or a reference crop such as alfalfa (ETr) with specific characteristics [20,21]. Importantly, ETr or ETo include a specific reference crop (alfalfa or grass, respectively). In this study, we define ETo to be the same as PET defined elsewhere in the literature (see Penman or Penman-Monteith, PM) and does not relate to a specific crop (defined in Irmak and Haman, 2003, https://doi.org/10.32473/edis-ae256-2003, accessed on 12 December 2022). The ETo is expected to be the maximum amount water transpired from a vegetative surface, and thus ETa, is a fraction of ETo. ETa is often compared to ETo to determine what fraction of maximum water use a vegetation community uses [32]. In this study, riparian ETa is calculated using ETo from gridded weather data as a substitute for ground-based weather station ETo from stations such as those in the Arizona Meteorological Network (AZMET) [33]. As explained in Nagler et al. (2020), weather station ETo data has been a key input to remotely sensed VI-based ETa algorithms that utilize various resolutions of imagery, for example the Moderate-resolution Imaging Spectrometer (MODIS) at 250 m or Landsat at 30 m spatial resolution [34].

1.2. General Methods as Applied to Terms

Climate parameters are used to predict ETo [20,21]. ETo is computed from weather data (see https://www.fao.org/3/x0490e/x0490e04.htm#reference%20crop%20evapotranspiration%20(eto); accessed on 27 July 2022). Weather stations report ETo because it captures the atmospheric water demand. Hunsaker et al., 2002 wrote FAO-56 procedures for alfalfa crop coefficients in the arid southwestern U.S. because the arid/semiarid climate greatly affects ETo estimation [35].

Despite these procedures for arid and semi-arid environments, in the Navajo Nation there are no long-term operational weather stations due to the inaccessibility of the region. Therefore, our estimations of ETa use a gridded representation of micro-meteorological variables. These two sources of weather data used are produced at different resolutions. The Daily Surface Weather and Climatological Summaries (Daymet) are at 1 km resolution [36,37], while the Parameter-elevation Relationships on Independent Slopes Model (PRISM) are at 4 km resolution [38–40]. We selected the 4 km resolution PRISM data because it is considered industry standard in regional climate studies. These gridded data are generated by the Daymet project (data are distributed by the ORNL-DAAC (https://daymet.ornl.gov/; accessed on 27 July 2022) and by PRISM (data are distributed by Oregon State (https://prism.oregonstate.edu/recent/; accessed on 27 July 2022).

In water resources management, and particularly in studies in the western U.S., a commonly used unit of measurement for water volumes is AF. To help understand uncultivated plant water use versus CU as a water volume in AF, Colorado State University provides easy-to-understand definitions of withdrawal for human and environmental needs [41], (https://waterknowledge.colostate.edu/water-management-administration/water-uses/; accessed on 27 July 2022). The definition of an AF is a measure of water volume equivalent one acre of land (about the size of a football field without the end zones) one foot deep or 325,851 gallons (1481 m^3) [41]. Approximately one AF serves the needs of two families for one year [41]. A water withdrawal refers to the quantity of water removed from a groundwater source or diverted from surface water to the point of use. CU is the portion of water withdrawal that is permanently removed from the immediate water environment by people, plants, or processes. Consumptive use volumes are often smaller than total withdrawals.

In this manuscript, CU takes the riparian plant area into account and is the annual water amount required to keep the ecosystem functioning properly. The plant water requirement is WD (ETa – PP) and is used to quantify CU (per area) in this dryland region where GDEs do not rely on PP and soil moisture storage is minimal. GDEs main resource for functioning is groundwater and not PP. Therefore, in this research, WD and CU are synonymous with groundwater discharge by vegetation in GDEs. Groundwater depth, surface runoff and land energy fluxes are inter-related and have well established feedbacks among them, and yet, they remain difficult to quantify, similarly to ETa in riparian ecosystems. One term in the study that should be described in more detail is what exactly remotely sensed measurements of ETa are measuring. A satellite pixel may include bare soil and vegetative cover whose signals are captured in the reflectance by bandwidth on the Landsat sensor. ETa requires a measure of vegetation density, either by leaf area index (LAI) or canopy cover and vegetation index (VI), which provide an estimate of vegetation greenness. ETa estimates may be underestimated if bare soil evaporation is not quantified accurately. Evaporation is considered to be minimal in drylands and transpiration is considered to be dominant for both phreatophytes and GDEs.

Maupin et al. (2018) describe the terms of water-use as: (1) water that is withdrawn from a source (groundwater or surface water, fresh or saline), (2) water that is delivered (domestic homes), (3) water that is unavailable (ETa, CU), and (4) water that is returned to a water resource via wastewater returns [42]. Along the Colorado River, water withdrawals are mainly for agriculture (78%), but also for other uses, such as public supply, domestic use, commercial use, industrial use, livestock and mining, aquaculture, wastewater returns, and power. A substantial portion of water withdrawal for crop irrigation is consumed via ETa, but when poorly managed, crops are not able to consume the entire portion of water applied. Usually, the majority of water withdrawal for crop irrigation is consumed via ETa, but some may become return flow to either surface or groundwater, which may become available to downstream users. As a result, return flow is created, either as surface flow or groundwater recharge, which is then used by other downstream users [42]. Natural resource managers and users of water accounting data for the Little Colorado River watershed are interested in accurate estimates of not only the weather data, among them PP and WD, but also and especially the water metrics, ETo and ETa, that are difficult to acquire for vast and mostly inaccessible landscapes. For over a decade the Navajo Nation and the Arizona Department of Water Resources have specifically been interested in CU across the riparian landscape along the Little Colorado River and select tributaries [43–45].

1.3. Objectives

In response to the interest in water metrics by stakeholders, this research addressed the challenge of acquiring meteorological data from the riparian study area as well as the larger geographic range, including most of northeastern Arizona, which lacks both meteorological data required to compute ETo as well as moisture flux tower data required to compute ETa at the ground-level. These two gridded datasets provide the two remote measurements of PP and ETo. We require these specific coarse, 1 km DayMet or 4 km PRISM, meteorological input data (PP and ETo) to derive the more difficult-to-measure riparian corridor ETa and WD per-pixel. The coarse resolution PP and ETo weather data is resampled to the Landsat 30 m resolution using a downsampling approach, where each 30 m pixel gets the PP and ETo value from the corresponding coarser resolution DayMet or PRISM.

The water resource managers from the Navajo Nation were specifically interested in acquiring one year of remotely sensed riparian corridor ETa and CU data to get an idea of the range of the water metrics that we estimated for the first time in this geographic region. With the use of Landsat 8/Operational Land Imager (OLI), we were able to provide four types of water balance data for a seven-year period from 2014–2020 covering northeastern Arizona. With the provided area estimate (acres and hectares) of riparian shrubs and trees within the specific region-of-interest (ROI) adopted by the Navajo Nation, we also extracted ETa and determined CU of riparian areas for the first time for this area. These specific tasks were addressed:

1. Acquire daily weather data from two gridded sources, Daymet (1 km) and PRISM (4 km) and Landsat 8/OLI (30-m) scenes that cover the northeastern corner of Arizona.
2. Calculate the daily ETo using the input weather data.
3. Standardize all computations to a 16-day time-step that matches the Landsat overpass dates to reduce outliers, then produce PP, ETo, ETa and WD.
4. Develop annual maps of PP, ETo, Eta, and WD water metrics at the Landsat 30 m spatial resolution.
5. Estimate riparian plant water use by three different and spatially explicit methods:
    i. a polygon-based 'hand-digitization' method of the riparian vegetative cover, and
    ii. a newly devised automatic rasterization method that counts any Landsat 30 m pixels containing vegetation as riparian using two levels of detail: a 'conservative' and 'best-approximation' to estimate the riparian area. The 'conservative' method considers only pixels with >50% of vegetation cover, the 'best-approximation' method considers any pixels with vegetation which results in a larger area estimate. We then calculate CU using any of the above methods for estimating riparian area.

The objective of this study was to establish a range of values for these water balance metrics for comparison, natural resource planning, and policymaking in the context of currently accepted and literature-reported estimates. Here, we hypothesize that our estimates of ETa and CU derived from gridded weather and remote sensing data will fall within the ranges reported and validated by the literature for similar regions.

2. Data and Methods

2.1. Study Area

For this study, we used a ROI that includes selected areas of riparian shrubs and trees along the Little Colorado River mainstem, its tributaries, streams, and nearby springs which exist on the Navajo Reservation and is within the Colorado River Lower Basin [46] (Figure 1). The ROI was created in ArcGIS by a contractor to Fred Phillips Consulting and provided to the authors of this study to meet some of the objectives outlined in Section 1.2. We provide image and numerical assessments of water metrics for the entire region encompassing the northeast corner of Arizona, USA. The entire study area contains the majority of the Navajo Nation as well as the entire Hopi Reservation.

Figure 1. The study region of interest (ROI) is comprised of the riparian corridors along the Little Colorado River tributaries and streams in the Navajo Nation.

Figure 1 shows the northeast corner of Arizona with the mainstem of the Little Colorado River in blue and the selected riparian vegetation of its tributaries, streams, and nearby springs in light and dark green for the ROI considered in this study. Riparian trees (dark green) and shrubs (light green) were delineated on high-resolution National Agricultural Imagery Program (NAIP) imagery (1 m resolution) from one summer image (June 2019) (see https://www.usgs.gov/centers/eros/science/usgs-eros-archive-aerial-photography-national-agriculture-imagery-program-naip, accessed on 27 July 2022) [47]. The high-definition polygon data for the riparian ROI comprised of shrubs and trees were scaled and gridded to Landsat-8/OLI satellite imagery (30 m resolution) using a rasterization algorithm that considers the full 30 m grid active if intersected by a tree or shrub from the polygon data.

We report values for four water metrics (ETo, PP, ETa, WD) for seven years (2014–2020) for the northeastern portion of Arizona. In order to provide estimates of CU, a variable that requires ground area, we used the ROI which is a vector-based digitized area of riparian vegetation along selected tributaries, streams and springs falling within the Navajo Reservation boundary.

2.2. Area Delineation of Riparian Trees and Shrubs

2.2.1. Vector-Based Riparian Area Delineation

We produced three types of area estimates of the riparian vegetation using different methods. These include one vector-based method and two raster-based methods. A range of estimates were produced for riparian shrubs and trees, and the corresponding total area, to show the sensitivity and range of values resulting from these different methods. The resolutions of the base imagery used in the vector-based method were different from the Landsat satellite imagery at 30 m resolution, as the NAIP scenes are 1 m resolution [47]. We illustrate how the riparian vegetation cover is estimated using the two sources of imagery, Landsat and NAIP.

For this study, we provide annual estimates of riparian area in hectares and acres for the ROI. CU estimates are confined to both riparian shrubs and trees on selected portions of the Navajo Nation. Furthermore, the total riparian vegetation area, which includes separate estimates for trees and shrubs, uses three ways of estimating area. Due to their significantly different physiography, we split the study area into the western and eastern halves (Figure 2). The various area estimates include the western trees, shrubs, and total riparian area, eastern trees, shrubs, and total riparian area, and the combined study area (i.e., western and eastern) for trees, shrubs, and total riparian area. We determined the annual estimates for four water metrics and for seven years for these nine distinct areas.

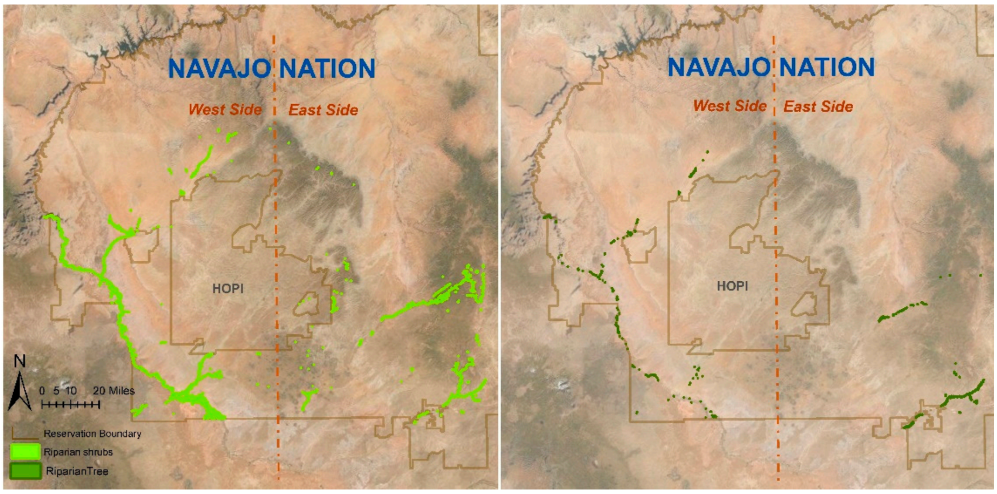

Figure 2. Digitized area showing riparian shrubs (left, light green) and trees (right, dark green) along select Little Colorado River tributaries and streams on the Navajo Nation that were delineated on a June 2019 high-resolution (1-m) National Agricultural Imagery Program (NAIP) scene.

Figure 2 shows the vector-based, digitized polygons that outline the riparian vegetation as shrubs (left, light green) and trees (right, dark green) using the one summer NAIP scene. The ArcGIS vector file is shown with a background image providing the landscape in the Northeast corner of Arizona with the boundary of both Navajo and Hopi Reservations. The digitized layer was the provided base-layer ROI from which the task of estimating CU for riparian cover progressed.

The vector-based riparian layer was hand digitized and was based on only one NAIP image. A large degree of human error was visible in the NAIP scene, which depicts a vast area, and most of the riparian corridor vegetation was not captured; this was an error that was propagated to the landscape scale (Figure 3). Despite the image being high resolution (1-m), the amount of riparian vegetation that was not digitized using the vector-based method resulted in an underestimation of acreage and consequently an inaccurate estimate of the water balance.

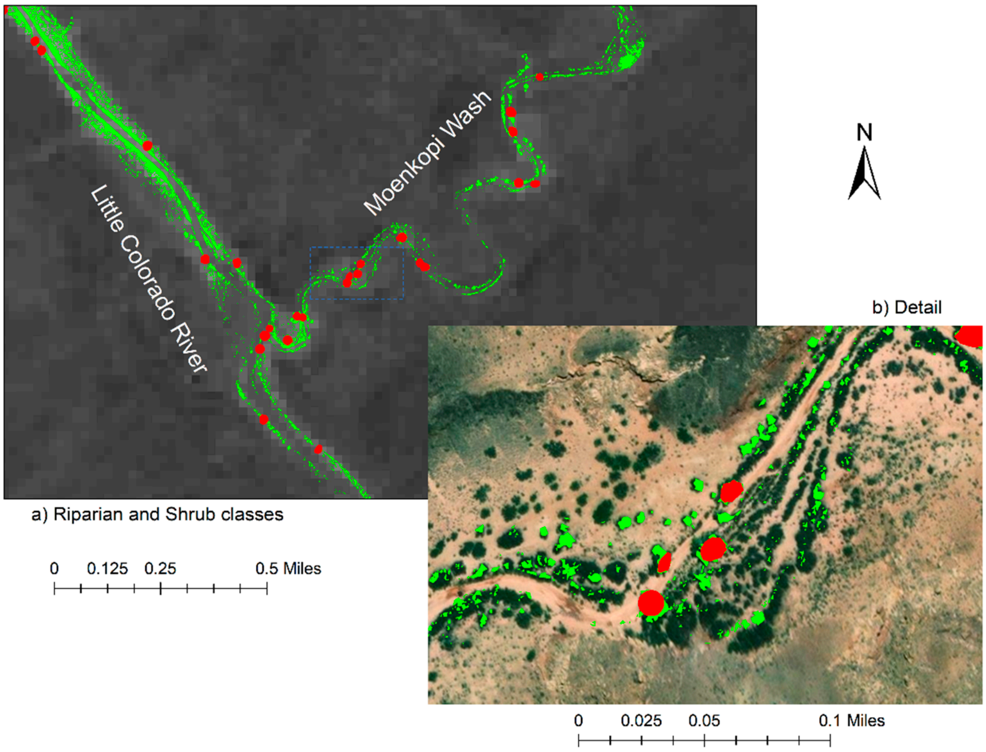

Figure 3. Digitization at two zoom levels depicting the vector-based method of delineating riparian shrubs (light green) and trees (red) along a selected portion of the Little Colorado River watershed based on a single summer 2019 National Agricultural Imagery Program (NAIP) image.

A high-definition outline of the study areas ROI was provided in the form of a geographic information system (GIS) vector data layer with riparian shrubs and trees digitized by following 1 m resolution, natural-color, NAIP imagery collected in the summer of 2019. The vegetation boundaries were delineated from this high-resolution imagery because during the peak growing season, plants are at their phenological maximum greenness and vigor (health) are more easily identifiable with remote sensing compared to dormant vegetation. The primary goal of delineating the naturally occurring uncultivated plant cover on the high-resolution imagery was to identify a plant community layer as one riparian grouping and to detect these separately as shrubs and trees. The reason for this classification was to determine whether native trees can be separated from non-native shrubs such as saltcedar to quantify separate water use estimates based on the ground cover This distinction is outside the scope of our study. This process of separating trees from shrubs was accomplished, but resulted in a large amount of green vegetation not detected, captured, or digitized perhaps due to the following: (i) a single NAIP image date was used and thus was unable to capture seasonality, (ii) the timing to capture the peak greenness of vegetation in the phenology cycle was missed, and (iii) the size of the imagery and area at 1 m resolution made the separation very challenging. This has led to serious underestimation of CU. To address this problem, we developed a raster-based method for estimating the riparian vegetation cover based on pixels from Landsat-8 OLI imagery (see Section 2.3). We provide results from both methods of area determination, with the caveat that the vector-based results are only a fraction of what we consider the actual riparian area. The digitized riparian shrubs and trees were necessary for producing a base-layer from which the rasterized estimates of area (calculated for both a 'conservative' and a 'best-approximation' area estimate) were used. The three area calculations resulted in three estimates of CU. Importantly, our raster-based CU estimates produced values that were congruent with the literature-based estimates published in 2020 [32].

2.2.2. Raster-Based Riparian Area Delineation

The manually derived vector outlines from the NAIP image were used to identify Landsat-8/OLI 30 m pixels that intersect any riparian vegetation. This process was further improved by comparison with high-resolution Google maps. The vector outline captured only a small fraction of existing riparian vegetation (see Figure 4). Figure 5 shows a riparian stretch comparing the two raster-based methods of capturing the riparian vegetation. To address the error in the vector-based method, the rasterizing algorithm expanded the original vector outline using first a 10 m buffer followed by a 50% inclusion threshold ('conservative'), then followed by including any intersection of a pixel with riparian vegetation ('best-approximation'). The two rasterized 30 m layers were created first using a 10 m buffer to aggregate the riparian vector area which was comprised of individual shrubs and trees before aggregating using the buffer mask of the separate digitized layers. The 'conservative' estimates were defined by whether the new buffered outline exceeded 50% of the grid cell, and if the condition was met, then the whole 30 m pixel is considered to contain riparian vegetation. The pixel was omitted if buffered outline was less than 50% of the grid cell. This rasterization method helped capture the riparian vegetation (Figure 4a, left). To expand the riparian area to be included in the 'best-approximation' area estimates, we enhanced this new raster riparian mask by relaxing the 50% threshold to include all intersections with pixels such that if the pixel intersected any riparian vegetation then it was included (Figure 4b, right).

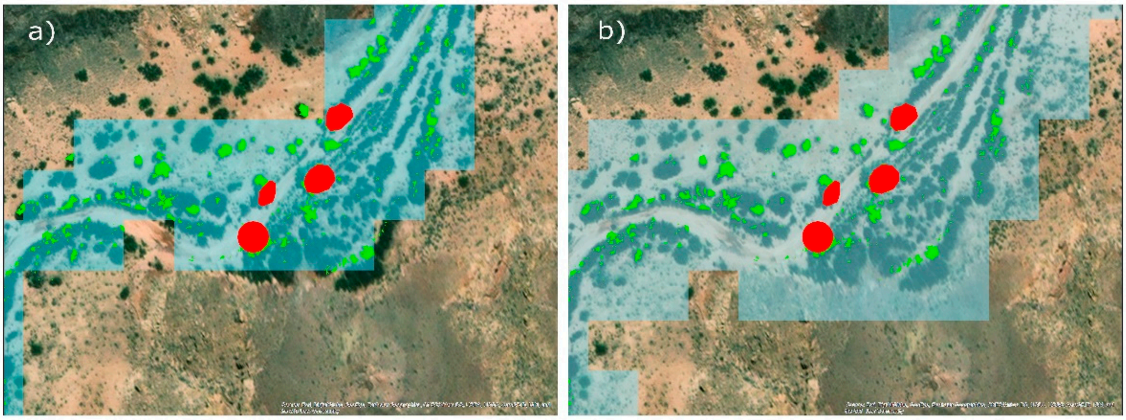

Figure 4. Riparian trees (red) and shrubs (light green) digitized using a June 2019 National Agricultural Imagery Program (NAIP) image and overlaid with light-colored, square, Landsat 30 m resolution pixels highlighting the raster-based method of counting riparian vegetation cover for the "conservative" ((**a**), left) and "best-approximation" ((**b**), right) area estimates.

2.3. Acquired Landsat-8/OLI Satellite Imagery

Figure 5 shows 11 Landsat-8/OLI scenes outlined in red that cover the entire Navajo Nation and include areas in southeastern Utah, northwestern New Mexico, and northeastern Arizona. The six images in green only show the images we used over the study region that overlap with the riparian corridors of the Little Colorado River and its tributaries and streams. The six Landsat 8/OLI scene Paths/Rows are 037/035, 036/035, 035/035, 037/036, 036/036 and 035/036.

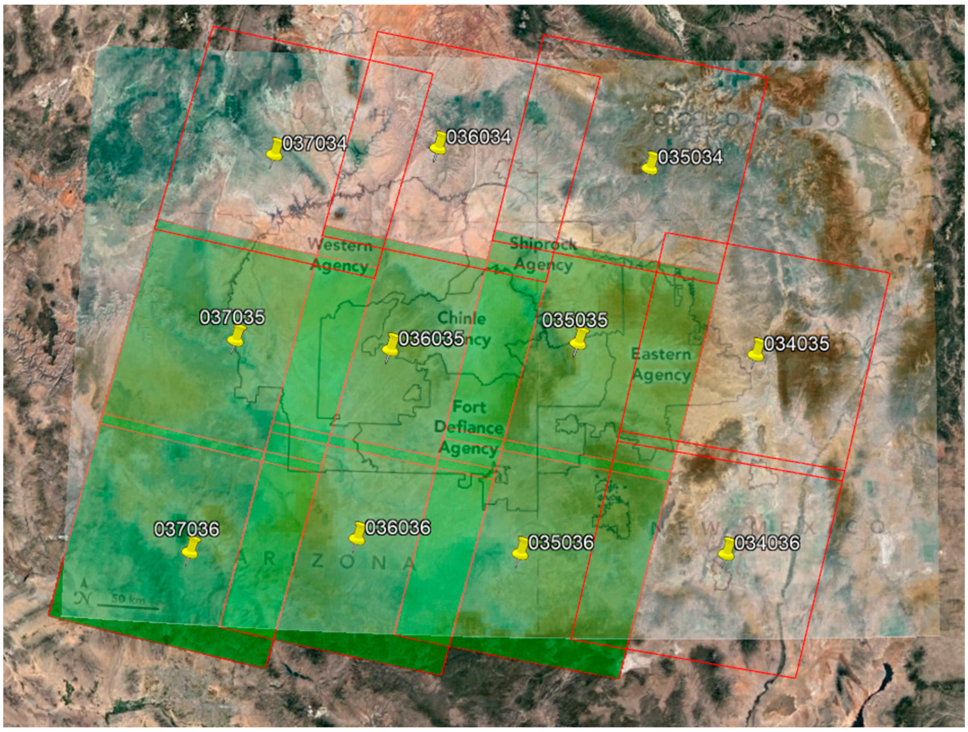

Figure 5. Image showing the extend of all 11 Landsat tiles outlined in red over the Navajo Nation in the northeastern corner of Arizona; only six Landsat scenes shaded in green with UTM labels overlay the riparian corridor ROI that was used in this study.

From these six Landsat-8/OLI scenes that cover the riparian corridor study area, we acquired time-series data for complete years, which is approximately 23-scenes per year for seven calendar (not water) years (2014–2020). Note that 2013 imagery was not acquired until part-way into the year or Cycle 10). In total, we acquired 161 images from the NASA/USGS Landsat distribution portal. The Landsat-8/OLI data were processed and filtered to remove any contamination from clouds, shadows, aerosols, and other atmospheric problems. Only select images for each year between 2014 and 2020 (Table 1) could be used based on quality standards. After selecting the atmospherically clear imagery, 156 images were further processed and filtered to compute the two-band Enhanced Vegetation Index (EVI2) at 16-day intervals following the simplified algorithm for EVI2 [48]. The algorithm is simpler because it does not require the blue band and performs better than EVI over bright targets, residual clouds, thick aerosol, and snow [49,50]. This study utilized only EVI2 to compute ETa for the same period.

2.4. Weather Data Acquisition on the Navajo Reservation

The ETa calculations provided in Equations (1) and (2) require an estimate of reference ETo, which is typically the maximum amount of water used by a full-cover crop such as alfalfa [20,21]. It is important to note that many factors, not just full-cover and a well-watered crop, govern ETo measurement accuracy [51]. Daily potential ET (ETo, mm/day) is computed with the Blaney-Criddle (BC) algorithm [52] and follows the FAO equation [53] https://www.fao.org/3/s2022e/s2022e07.htm#3.1.3%20blaney%20criddle%20method, accessed on 25 July 2022 described below in Equation (1) [52,53]:

$$ETo\ \text{(Blaney-Criddle)}: P \times (0.457 \times T_{mean} + 8.128) \quad (1)$$

where ET_o is the reference evapotranspiration [mm/day]; T_{mean} is the mean daily temperature [°C] given as $T_{mean} = (T_{max} + T_{min})/2$; P is the mean daily percentage of annual daytime hours [53].

Table 1. The number of satellite images acquired from NASA/USGS Landsat OLI (2014 to present), and for this study, only scenes for each year between 2014 and 2020 were used in this study.

Cycle	2013	2014	2015	2016	2017	2018	2019	2020
1		5	8	11	13	16	3	6
2		21	24	27	29	32	19	22
3		37	40	43	45	48	35	38
4		53	56	59	61	64	51	
5		69	72	75	77	80	67	70
6		85	88	91	93	96	83	86
7		101	104	107	109	112	99	102
8		117	120	123	125	128	115	118
9		133	136	139	141	144	131	134
10	146	149	152	155	157	160	147	150
11	162	165	168	171	173	176	163	166
12	178	181	184	187	189	192	179	182
13	194	197	200	203	205	208	195	198
14	210	213	216	219	221	224	211	214
15	226	229	232	235		240	227	230
16	242	245	248	251	253	256	243	246
17	258	261	264	267	269	272	259	262
18	274	277	280	283	285	288	275	278
19	290	293	296	299	301	304	291	294
20	306	309	312	315	317	320	307	
21	322	325	328	331	333	336	323	326
22		341	344	347	349	352	339	342
23	354	357	360	363	365			358

There were no obvious data sources for ETo near the riparian ROI. A few meteorological stations in Arizona were investigated through The Arizona Meteorological Network [33] (https://ag.arizona.edu/azmet/, accessed on 27 July 2022) but there were no stations within a reasonable distance to the ROI. Other weather data listed by the National Oceanic and Atmospheric Administration (NOAA) National Centers for Environmental Information (NCEI, https://www.ncei.noaa.gov/, accessed on 27 July 2022) [54] were found to be present in nearby places where weather stations exist, such as Blanding, Hopi, Page, Painted Desert, Meteor Crater, Winslow, Wupatki, Kayenta. These stations were not used because the stations do not span the topography of our study area and are temporally sparse for the time period between 2014–2020.

We used gridded products in the BC equation for riparian water use for the first time because we could not find reliable ground-based weather data. The gridded 1 km Daymet datasets [36,37] (see https://daymet.ornl.gov/; accessed on 27 July 2022) are accurate and provide a fine resolution weather data source for calculating ETo required in the Nagler ET(EVI2) equation modified using Landsat (Equation (2) [34]. Another alternative is the PRISM dataset (https://prism.oregonstate.edu/recent/, accessed on 27 July 2022) [40], however, these gridded data are coarser at four times the resolution, 4 km [39,40]. In this study, we decided on using both gridded products to provide rainfall and temperature data (mean, maximum and minimum values) required for computing PET as BC ETo.

2.5. Vegetation Index-Based Evapotranspiration Estimation

The estimates in this study are based on using EVI2 in the computation of ETa following the Nagler ET(EVI2) algorithm for riparian plant species [34]. A key component of determining ET(EVI2) is ETo. The daily ETo was determined from temperature and rainfall (T_{mean}, T_{max}, T_{min}, and P) from two sources, Daymet (1 km) [37] and PRISM (4 km) [38–40] data. These daily ETo were averaged over each 16-day period to coincide with the Landsat-8/OLI image, using the 8 days before- and 8 days after- the Landsat overpass date. This 16-day average ETo corresponds to the same cycle period for which ETa is calculated.

EVI2 is nearly identical to EVI as measured over riparian corridors [34]. In the original water use equation, measurements of ETa from flux towers in riparian corridors were scaled to the landscape using the MODIS satellite sensor and the EVI [22]. In this research, the ETa equation used had been improved in previous studies with the addition of ground-based data sources of water use such as from sap flow sensors [24]. The transpiration measurements were then scaled to estimate water use for the river reach, or wider area, using satellite-derived EVI [25]. River reach estimates of plant water use are especially useful when the uncultivated landcover has been mapped into separate vegetation classes [28]. An empirical equation based on crop coefficients and EVI was produced, applied [30] and scaled [31] to the Lower Colorado River agricultural districts and adjacent uncultivated vegetative areas to improve upon the existing USBR-LCRAS methods [27]. The crop-coefficient form of this ETa algorithm was improved again in 2013 [55] using a revised and updated equation in the form of $ET_a = ET_o\,[a(1 - e^{-bEVI}) - c]$ where the term $(1 - e^{-bEVI})$ is derived from the Beer-Lambert Law to express light absorption by a canopy and EVI replaces leaf area index as an estimate of the density of light-absorbing units. The resulting algorithm predicted ET_a across both riparian plants and crops ($r^2 = 0.73$) [55] and although we do not use MODIS in this study, we follow the format of this original algorithm that is described in Equation (2) [55]:

$$ET_{a\,(MODIS)}: ET_{o\,(daily)} \times 1.65(1\text{-}e^{-2.25EVI}) - 0.169 \quad (2)$$

ETo = potential evapotranspiration (PET) for the area

$$EVI = G\,(\rho NIR - \rho Red)/(\rho NIR + C1 \times \rho Red - C2 \times \rho Blue + L)$$

where G is the gain factor (set at 2.5), C1 and C2 correct for aerosol resistance (=6 and 7.5, respectively), L adjusts for canopy background (=1), and ρNIR, ρRed, ρBlue are reflectance in the near infrared, red, blue wavelengths, respectively [56,57].

This ETa Equation (2) was tested against water balance data for five irrigation districts and flux tower data for two riparian zones for which season-long or multi-year ET_a data were available [55]. Predictions were within 10% of measured results in each case, with a non-significant ($p = 0.89$) difference between mean measured and modeled ET_a of 5.4% over all validation sites [55], which is why we selected this form of the ETa equation to use in this research.

Most riparian corridors are narrow; the use of MODIS for measurement and monitoring of these areas is often questioned regarding its usefulness to monitor riparian plant trends using VI and predict ETa for these riparian areas given its pixel size of 250-m. Jarchow et al., 2017a,b used the relatively higher resolution Landsat imagery (30-m) to study the change in the Normalized Difference Vegetation Index (NDVI) and ETa based on scaled NDVI in the riparian corridors of the Colorado River delta [58,59]. They then compared MODIS-derived EVI to Landsat-8/OLI [60]. Using the original algorithm from MODIS, Equation (2), and this modified equation using Landsat, Equation (3), Nagler et al., 2020 directly compared ETa for 20 years from 2000 to 2019 for the Lower Colorado River delta with very little difference in ETa measured between the two sensors [34]. The use of the relatively higher resolution imagery from Landsat-8/OLI was selected for use in other studies of the Lower Colorado River's riparian plant community change in greenness and water use [7]. For this study of the Little Colorado River's riparian consumptive use, we use ETa measured from Landsat-8/OLI only, following Equation (3):

$$ET_{a\ (Landsat)}: ET_{o\ (daily)} \times 1.65(1\text{-}e^{-2.25EVI}) - 0.169\ [\text{-}] \quad (3)$$

In this study, the EVI2 replaces EVI in the ETa algorithms (Equations (2) and (3)). EVI2 is a proxy for vegetation greenness and was computed from 16-day Landsat-8/OLI data as was done in recent riparian trend research [7,34]. EVI2 is preferred in cases when the data quality is high and atmospheric effects are insignificant (i.e., our study area). EVI2 is the simplified two-band version of Equation (2) and is computed as follows in Equation (4):

$$EVI2: 2.5 \times (NIR - RED)/(NIR + 2.4 \times RED + 1.0) \quad (4)$$

We then computed the average annual ETa (mm/year) for all years and averaged using the seven years (2014–2020). We derived ETa following recently published methods [7] but substituted gridded ETo data instead of ground-based weather station ETo. We computed ETa using two sources of ETo data: one from Daymet following Equation (5) and the other from PRISM following Equation (6).

$$ET_{a\ (Landsat)}: ET_{o\ (daily)\ (Daymet)} \times 1.65(1\text{-}e^{-2.25EVI2}) - 0.169 \quad (5)$$

$$ET_{a\ (Landsat)}: ET_{o\ (daily)\ (PRISM)} \times 1.65(1\text{-}e^{-2.25EVI2}) - 0.169 \quad (6)$$

Water metrics (mm/year), which include PP, BC ETo, ETa, WD, and CU based on area-estimates, were computed for each year in the study period (2014–2020).

2.6. A West:East Divide for Weather Data on the Navajo Nation

To refine the analysis and capture any potential climate and/or elevational gradient sensitivity we divided the study area into West and East halves because of differences in the physical geography. There are higher elevations (e.g., mountains) on the East side of the study area compared to the West side, and these geographic differences result in different weather patterns. Because substantial differences exist between the eastern and western halves, we separated our water metric values into East and West and plotted standardized anomalies (ratio of difference and standard deviation) for the two sides separately in addition to showing the average results for the full area. Standardized anomalies capture not only geographic differences in water metrics by year but also capture variations by type (shrubs and trees).

3. Results

3.1. Area Determinations and Literature-Based Estimates

These data present the first-ever Landsat-based, 30 m resolution, estimates of the water balance of the northeast Arizona region, including ETa calculated using gridded weather data products for the input variables to the Nagler ET(EVI2) algorithm [7,34,61], and CU estimates for riparian corridors along the Little Colorado River and its tributaries, streams and springs in this vast and generally inaccessible part of the Navajo Nation's watershed (Figure 1). The data analysis could not be performed without first mosaicking and filtering (e.g., cloud, shadows, etc.) the Landsat-8/OLI scenes. These images were processed into EVI2 and ETa using Equations (4) and (5). Our estimates were based on three sources of data: (i) detailed digitized riparian plant cover, (ii) gridded weather information (e.g., Daymet and PRISM), and (iii) USGS/NASA Landsat-8/OLI satellite imagery of six scenes from each of seven years. We provide maps and tabular estimates of water metrics for seven years (2014–2020) depicting their annual means and standard anomalies. The key values utilized in this study are provided (Tables 2 and 3) with all data reprocessed to 30 m over the riparian corridor ROI of the tributaries, streams and springs of the Little Colorado River.

Table 2. Riparian area estimates divided into the West (top), East (middle) and Total (merged) (bottom) using three methods for totaling the riparian vegetation land cover area.

	'Conservative' Raster 30 m		'Best-Approximation' Raster 30 m		Digitized Polygons	
Western Area	Hectares	Acres	Hectares	Acres	Hectares	Acres
Riparian Tree	119.7	295.8	240.48	594.2	40.2	99.4
Shrub	14,978.6	37,012.9	19,629.81	48,506.2	3640.2	8995.1
Subtotal	15,098.3	37,308.7	19,870.29	49,100.5	3680.4	9094.5
Eastern Area	Hectares	Acres	Hectares	Acres	Hectares	Acres
Riparian Tree	447.3	1105.3	707.0	1746.9	155.9	385.3
Shrub	3816.8	9431.5	5037.6	12,448.1	1137.7	2811.3
Subtotal	4264.1	10,536.8	5744.5	14195.0	1293.6	3196.6
Total Area	Hectares	Acres	Hectares	Acres	Hectares	Acres
Riparian Tree	567.0	1401.1	947.4	2341.1	196.2	484.7
Shrub	18,795.4	46,444.4	24,667.4	60,954.3	4777.9	11,806.4
Total	19,362.4	47,845.5	25,614.8	63,295.5	4974.0	12,291.1

Table 3. Reproduced literature-based riparian water metric estimates for different vegetation density, cover and ETo (shaded green) from various study sites in Arizona [32] for comparison to estimed data (this report) for ETo, ETa, PP, WD and CU.

Riparian Vegetation Type	ETo or ETa (mm/Year)	ETo or ETa (in/Year)	Rainfall (in/Year) *Bresloff et al., 2013	Net Water Requirement (in/Year) (No Soil Moisture Change)	ETo or ETa (ft/ Year)	Net Water Requirement (ft)	Area (Acres)	Consumptive Water Use (Acre-ft)
Average Riparian Cover Reach Level	684	26.93	6.06	20.87	2.24	1.74	14,598	25,387
Riparian Gallery Trees Only	1123	44.21	6.06	38.14	3.68	3.18	14,598	46,397
Navajo Nation Potential ET (ETo)	1473	57.99	6.06	51.93	4.83	4.33	14,598	63,258
Lower Colorado River, Potential ET (ETo)	2021	79.57	6.06	73.51	6.63	6.13	14,598	89,486
NRCE Report	1273	50.1	5.10	45.0	4.18	3.75	26.2	98.4
NRCE Report Potential ET (ETo)	2080	81.9	8.1	73.8	6.83	6.15	-	108.2

Area estimates are provided for all three methods, by trees, shrubs and their totals, and for the western, eastern and total area ROI (Table 2). We report results by the vector-based area estimates 'digitized polygons' only for contrast purposes compared to the more realistic rasterized method estimates. In Table 2, the first two headings are rasterized areas that used 30 m resolution pixels and were determined by inclusion methods: (i) Raster 'conservative'—which used pixels with 50% of the intersections with the buffered area, (ii) Raster 'best-approximation'—which used pixels with all intersections with the buffered area; and (iii) Digitized Polygons of riparian trees and shrubs created in ArcGIS.

We report our data findings (PP, ETo, ETa, WD, CU) based on our two rasterized calculation methods to estimate area ('conservative' and 'best-approximation') and the digitized riparian vector layer to produce water metrics based on area of riparian vegetation. The two raster methods resulted in more riparian ground cover than the digitized areas that only captured individual shrubs and trees. Therefore, our conclusions provide a range for our water balance values, and they are based only on the 'conservative' and 'best-approximation' rasterized areas in Table 2.

In Table 2 we provide the areas from which we calculate the water metrics. Using the rasterizing algorithm created for this study, the area considered 'best-approximation' for riparian trees was 947 ha (2341 acres) and the 'conservative' estimation for trees was 567 ha (1401 acres), while the digitized riparian area included only a fraction of the actual area, estimated to be 196 ha (485 acres), or 21% to 35% of the 'best-approximation' and 'conservative' rasterized estimates, respectively. The 'conservative' rasterized area for shrubs was estimated to be 18,795 ha (46,444 acres); for the 'best-approximation' estimate, the shrubs area was 24,667 ha (60,954 acres), while the digitized area for shrubs was 4778 ha (11,806 acres) or 19% to 25% of the rasterized estimates. Due to the very few trees digitized, the riparian shrub estimates were close in area to the total riparian corridor estimates. For the total riparian corridor, we estimated the 'best-approximation' area using 30 m pixels to be 25,615 ha (63,296 acres). In comparison, the 'conservative' area was 19,362 ha (47,845 acres) and for the area using only digitization, the area was only 4974 ha (12,291 acres) or 19% to 26% of the rasterized estimates.

The main difference between the western and eastern halves of the Navajo Nation is that the west is lower in elevation, drier and has more extensive riparian vegetation cover. The western area contains 19,870 ha (49,100 ha) of riparian vegetation cover compared with only 5745 ha (14,195 acres) in the east (Table 2). Thus, approximately 70% of the total riparian vegetation is in the west; this has direct impacts on the estimate of the PP, ETa, WD and the CU for each area.

Prior to estimating the riparian corridor ROI area in this study, we were tasked with using only reviewed literature to estimate both ETa and CU for uncultivated riparian vegetation. The range of values for pertinent water metrics that were predicted in the initial study were based on estimates derived from studies of other riparian corridors and not the Little Colorado River watershed; these were gathered from literature estimates and summarized in Table 3 by Nagler, 2020 [32]. Table 3 shows predicted ETa, PP, the net water requirement or water deficit (WD) and CU based on a given area of 14,598 acres, the initial estimate for total area of the Little Colorado's riparian vegetation. Importantly, Table 3 includes a study by the Natural Resources Consulting Engineers (NRCE) based on only 26 acres of riparian vegetation on the Hopi Reservation [45] which is contrasted with the other literature estimates summarized in the 2020 report [32]. At the time that Table 3 was created, the Arizona Department of Water Resources (ADWR) preliminary study identifying greater areas of riparian vegetation was not available for inclusion in the literature review [32]; however, the results from this larger region are compared and contrasted to our findings in the discussion. ETo, the maximum amount of available water used by plants, estimates were similar to the Hopi Tribe report [43] and Lower Colorado River studies, but they resulted in different CU values because the plant water requirements for shrubs and tree cover and the respective total areas were different. The ETo estimated from studies on the Navajo Nation showed a nearly 3/4 lower ETo of 1473 mm/year (4.83 ft) compared with the Lower Colorado studies showing ETo of 2021 mm/year (6.13 ft) resulting in a CU estimate of 63,258 AF. Based on these literature estimates, riparian shrubs would consume 25,387 AF and gallery forests would consume 46,397 AF (Table 3). The CU literature-based estimates are from the riparian plant water requirement, also called water demand or water deficit (WD), which was 1.74 ft for shrubs and 3.18 ft for trees (Table 3). Our study using the vector methods show a WD ranging between 0.57–0.91 ft (1/3 lower compared to literature values in Table 3) and a lower digitized area of 12,291 acres, resulting in a CU of 7182 acre-ft, much lower than this literature-based range of 25,387–46,397 acre-feet (Table 3). By comparison, our study estimates an ETo of 4.09 feet and results in a CU of 50,300 acre-ft. These lower measured results are primarily due to the fraction of trees being only 4.1% of the riparian plant cover, with shrubs being 95.9% of the riparian corridor as determined from the digitized ROI layer. Since this ROI discrimination method did not capture the riparian vegetation fully, we calculate these water metrics using raster methods.

3.2. West:East Divide Based on Physiography and Weather Data across the Navajo Nation

A summary of the results is provided for the ETo, ETa, PP and WD; this data is divided into shrubs, trees and the total riparian vegetation, for each year, with the mean and standard deviation data (based on the seven years, 2014–2020) and is split into Tables 4 and 5 in order to demonstrate the different values between the two halves of the Navajo Nation study area (Table 4) and as a whole region (Table 5).

Table 4. Water metrics (ETo, ETa, PP, WD) using Daymet gridded weather data (1 km) and Landsat for each year, their mean and standard deviation, calculated for the riparian ROI by ground area for shrubs, trees, and total riparian vegetation divided into the West (top) and East (bottom) sides of the study area within the Navajo Nation.

West	**DAYMET Dataset**											
	Shrub (mm/Year)				**Riparian (mm/Year)**				**Total (mm/Year)**			
Year	**ET0**	**ETa**	**PP**	**WD**	**ET0**	**ETa**	**PP**	**WD**	**ET0**	**ETa**	**PP**	**WD**
2014	1561.4	409.4	174.3	235.1	1564.1	596.9	163.8	433.1	1560.7	411.7	174.2	237.5
2015	1515.0	354.1	358.2	−4.1	1513.3	542.3	388.1	154.2	1513.4	356.4	358.5	−2.1
2016	1506.9	378.8	269.0	109.9	1515.4	542.4	303.7	238.7	1506.3	380.8	269.4	111.4
2017	1524.4	383.5	200.6	182.9	1531.5	554.0	259.0	295.0	1526.2	385.6	201.3	184.3
2018	1518.0	392.6	264.0	128.6	1521.7	628.2	266.2	362.0	1517.5	395.5	264.1	131.4
2019	1502.8	416.6	210.3	206.3	1504.5	558.1	217.7	340.4	1505.1	418.3	210.4	208.0
2020	1568.7	476.0	92.0	384.0	1576.3	595.8	90.4	505.3	1568.1	477.4	92.0	385.4
Mean	1528.2	401.6	224.1	177.5	1532.4	573.9	241.3	332.7	1528.2	403.7	224.3	179.4
Stdev	26.3	38.7	83.9	120.2	27.3	33.2	96.3	117.6	25.8	38.4	84.0	120.1
East	**DAYMET Dataset**											
	Shrub (mm/Year)				**Riparian (mm/Year)**				**Total (mm/Year)**			
Year	**ET0**	**ETa**	**PP**	**WD**	**ET0**	**ETa**	**PP**	**WD**	**ET0**	**ETa**	**PP**	**WD**
2014	1364.0	456.7	252.3	204.4	1401.0	532.8	218.4	314.5	1368.6	466.1	248.1	218.0
2015	1337.0	370.7	471.2	−100.5	1375.8	431.7	367.7	64.0	1341.7	378.2	458.4	−80.3
2016	1336.6	417.6	317.3	100.3	1368.8	483.9	274.6	209.3	1340.5	425.8	312.0	113.8
2017	1355.5	503.6	276.6	227.0	1385.9	508.3	218.3	290.1	1359.2	504.2	269.4	234.7
2018	1338.2	478.9	268.8	210.1	1367.9	526.1	252.2	273.9	1341.9	484.7	266.8	217.9
2019	1315.1	507.6	337.6	170.0	1346.9	574.7	262.0	312.6	1319.0	515.8	328.3	187.5
2020	1376.8	527.0	207.4	319.6	1409.9	550.4	201.5	348.9	1380.9	529.9	206.7	323.2
Mean	1346.2	466.0	304.5	161.6	1379.4	515.4	256.4	259.1	1350.3	472.1	298.5	173.5
Stdev	20.6	55.6	84.9	132.9	21.4	46.9	55.8	96.3	20.7	53.9	81.1	128.0

Table 5. Water metrics (ETo, ETa, PP, WD) using Daymet gridded weather data (1 km) and Landsat for each year, their mean and standard deviation, calculated for the riparian ROI by ground area for shrubs, trees, and total riparian vegetation for the full study area within the Navajo Nation.

Total Area	**DAYMET Dataset**											
	Shrub (mm/Year)				**Riparian (mm/Year)**				**Total (mm/Year)**			
Year	**ET0**	**ETa**	**PP**	**WD**	**ET0**	**ETa**	**PP**	**WD**	**ET0**	**ETa**	**PP**	**WD**
2014	1521.1	419.1	190.2	228.8	1442.4	549.1	204.5	344.6	1517.6	423.9	190.8	233.1
2015	1478.7	357.5	381.3	−23.8	1410.7	459.8	372.9	86.9	1474.9	361.3	380.9	−19.7
2016	1472.1	386.7	278.8	107.9	1406.0	498.7	281.9	216.8	1469.1	390.9	278.9	112.0
2017	1489.9	408.0	216.1	191.9	1422.8	519.9	228.6	291.3	1488.7	412.2	216.6	195.6
2018	1481.3	410.2	265.0	145.2	1407.0	552.0	255.7	296.3	1478.1	415.5	264.7	150.8
2019	1464.4	435.2	236.3	198.9	1386.9	570.4	250.8	319.7	1463.3	440.2	236.8	203.4
2020	1529.5	486.4	115.6	370.8	1452.1	561.9	173.3	388.6	1526.1	489.2	117.7	371.5
Mean	1491.0	414.7	240.5	174.3	1418.3	530.3	252.5	277.7	1488.3	419.0	240.9	178.1
Stdev	24.8	40.2	82.3	120.4	22.6	39.8	63.9	99.3	24.4	40.0	81.6	119.4

Table 4 shows the results from the gridded 1 km Daymet weather data, the higher resolution of the two gridded datasets, as input for calculating the four water metrics shown, ETo, ETa, PP, and the WD for the West (top) and East (bottom). The ETa for vegetation in the West has a mean for shrubs of 401.6 mm/year, for trees of 573.9 mm/year, and for a total riparian area of 403.7 mm/year. Note that the total is not significantly different than the shrub values because the riparian corridor area is predominantly shrub cover. The ETa for the vegetation in the East was 466.0 mm/year for shrubs and 515.4 mm/year for trees, and for the total riparian area ETa was 472.1 mm/year (Table 4). Rainfall for the West measured for the total riparian area is 224.3 mm/year, but in the East it is 298.5 mm/year. WD was calculated pixel by pixel and averaged over the region but were simply subtracted from the previous two columns, ETa − PP (Table 4). The WD averages between the West (179.4 mm/year) and the East (173.5 mm/year) are close, with the West having a slightly higher value by 5.9 mm/year. Plants are using 26% of ETo in the West and 35% of ETo in the East. Note that in the year 2015 there was more PP than ETa resulting in a negative shrub water requirement, which affected estimates of CU in both the West and the East; it had a greater effect in the East, and thus impacted the joint area shown in Table 5.

Table 5 shows the results across the entire Navajo Nation study area (combined West and East sides) from the gridded 1 km Daymet weather data as input for calculating the four water metrics. The whole riparian corridor has a mean ETa for shrubs of 414.7 mm/year and for trees of 530.3 mm/year, and for both riparian covers ETa was 419.0 mm/year or 28% of the ETo (Table 5). Rainfall (PP) for the shrub part of the corridor was 240.5 mm/year and for trees it was 252.5 mm/year, and for both it was 240.9 mm/year (Table 5). The trees contributed so little because they represented such a small area that was dominated by shrubs, making the estimates of ETa for shrubs and the total area very close in their value. This also holds true for the plant water requirement, the WD estimates, for the full area. The WD for shrubs had a mean of 174.3 mm/year and a mean of 277.7 mm/year for trees, while the mean WD for the total riparian area was 178.1 mm/year (Table 5). Similar to the method applied in compiling Table 4 data, WD was calculated pixel by pixel, and averaged over the region from the mask; however, instead of showing both columns in this table, we report the values that were simply subtracted from the previous two columns, ETa – PP. It is important to note that the average WD for trees is 103.4 mm/year greater than for shrubs. Overall, the riparian species are only using 28% of the available water, ETo.

Table 6 also shows water metric data for the riparian ROI West–East division and the total study area within the Navajo Nation. The ETa is provided in mm/year, inches/year and feet/year. The PP and WD are in inches/year. The WD is also provided in feet. Note that WD is equivalent to the Net Water Requirement by the plants in the riparian corridor and can be compared to Table 3 columns 5 and 7; the dominant cover is by shrubs, not trees, yet trees have a greater water requirement or WD. The WD is multiplied by the area or acreage to produce the estimate of CU in acre-feet. We used gridded Daymet weather data (1 km) and Landsat (30-m) to measure these metrics as the annual mean of seven years (2014–2020) using the rasterized 'conservative' method. The CU is calculated by ground area for shrubs, trees, and total riparian vegetation for the West, East and Combined total study area of the Little Colorado River and its tributaries, streams and springs on the Navajo Nation. The West CU 'conservative' estimate is 24,885 AF and the East CU 'conservative' estimate is 6763 AF. The combined total area (West and East) CU 'conservative' estimate is 31,648 AF. The ETo is provided in the last row (shaded, blue). ETa is approximately 30% of the ETo. The CU based on ETa (31,648 AF) is approximately 16% of CU based on ETo (195,802 AF) (Table 6).

Table 6. Final water metric results for the riparian ROI showing the rasterized 'conservative' estimate of the mean data from 2014 to 2020 using gridded Daymet weather data (1 km) and Landsat (30-m) to derive ETa (mm, in, ft), PP (in), WD (in, ft) and ETo (mm, in, ft) (last row); the CU (acre-ft, last column) is calculated by ground area for shrubs, trees, and total riparian vegetation.

ETa (mm/Year)	ETa (in/Year)	PP (in/Year)	WD (in/Year)	ETa (ft/Year)	WD (ft/Year)	Area (Acres)	CU (Acre-ft)
Shrubs, West							
424.01	16.69	8.70	7.99	1.39	0.67	37,012.9	24,655.8
Trees, West							
626.70	24.67	9.36	15.32	2.06	1.28	295.8	377.5
West Subtotal							
424.33	16.71	8.70	8.00	1.39	0.68	37,308.7	24,885.0
Shrubs, East							
490.11	19.30	11.71	7.59	1.61	0.63	9431.5	5963.8
Trees, East							
538.45	21.20	10.06	11.14	1.77	0.93	1105.3	1025.8
East Subtotal							
491.96	19.37	11.67	7.70	1.61	0.64	10,536.8	6762.9
Combined							
Full Area Shrubs							
437.43	17.22	9.31	7.91	1.44	0.66	46,444.4	30,619.6
Full Area Trees							
557.08	21.93	9.91	12.02	1.83	1.00	1401.1	1403.3
ETa Navajo Nation Riparian ROI Total							
439.22	17.29	9.35	7.94	1.441	0.661	47,845.5	31,647.9
ETo Navajo Nation Riparian ROI Total							
1488.27	58.59	9.35	49.24	4.883	4.092	47,845.5	195,801.6

Table 7 also shows water metric data for the riparian ROI West–East division and the total study area within the Navajo Nation. In this table, we also used gridded Daymet weather data (1 km) and Landsat (30-m) to measure these metrics as the annual mean of seven years (2014–2020) using the rasterized 'best-approximation' method. We measured these metrics as the annual mean of seven years (2014–2020). The West CU 'best-approximation' estimate is 28,901 AF and the East CU 'best-approximation' estimate is 8082 AF. The combined total area (West and East) CU 'best-approximation' estimate is 36,983 AF. The ETo is provided in the last row (shaded, blue). ETa is approximately 28% of the ETo. The CU based on ETa (36,983 AF) is approximately 14% of CU based on ETo (259,029 AF) (Table 7).

Table 7. Final water metric results for the riparian ROI showing the rasterized 'best-approximation' estimate of the mean data from 2014 to 2020 using gridded Daymet weather data (1 km) and Landsat (30-m) to derive ETa (mm, in, ft), PP (in), WD (in, ft) and ETo (mm, in, ft) (last row); the CU (acre-ft, last column) is calculated by ground area for shrubs, trees, and total riparian vegetation.

ETa (mm/Year)	ETa (in/Year)	PP (in/Year)	WD (in/Year)	ETa (ft/Year)	WD (ft/Year)	Area (Acres)	CU (Acre-ft)
Shrubs, West							
401.58	15.81	8.82	6.99	1.318	0.582	48,506.2	28,250.15
Trees, West							
573.95	22.60	9.50	13.10	1.883	1.091	594.2	648.59
West Subtotal							
403.67	15.89	8.83	7.06	1.324	0.589	49,100.5	28,900.52
Shrubs, East							
466.01	18.35	11.99	6.36	1.529	0.530	12,448.1	6597.76
Trees, East							
515.43	20.29	10.09	10.20	1.691	0.850	1746.9	1484.70
East Subtotal							
472.09	18.59	11.75	6.83	1.549	0.569	14,195.0	8082.43
Combined							
Full Area Shrubs							
414.74	16.33	9.47	6.86	1.361	0.572	60,954.33	34,847.91
Full Area Trees							
530.28	20.88	9.94	10.93	1.740	0.911	2341.15	2133.29
ETa Navajo Nation Riparian ROI Total							
419.01	16.50	9.49	7.01	1.375	0.584	63,295.48	36,982.95
ETo Navajo Nation Riparian ROI Total							
1488.27	58.59	9.49	49.11	4.883	4.092	63,295.48	259,028.65

Table 8 also shows water metric data for the riparian ROI West–East division and the total study area within the Navajo Nation. However, in this table, we used the vector-based method of 'digitized polygons' to estimate the area. This table provides the estimates using Daymet weather data (1 km) and Landsat (30-m) to measure the water metrics using the annual mean of seven years (2014–2020). Using the vector-based method, the West CU estimate is 5353 AF and the East CU estimate is 1820 AF. The combined total area (West and East) provided using CU estimated using 'digitized polygons' is 7182 AF. This method produced the lowest values. The ETo is provided in the last row (shaded, blue). ETa is approximately 28% of the ETo. The CU based on ETa (7182 AF) is approximately 14% of CU based on ETo (12,291 AF) (Table 8).

Table 8. Final water metric results for the riparian ROI showing the vector-based method of 'digitized polygons' of the mean data from 2014 to 2020 using gridded Daymet weather data (1 km) and Landsat (30-m) to derive ETa (mm, in, ft), PP (in), WD (in, ft) and ETo (mm, in, ft) (last row); the CU (acre-ft, last column) is calculated by ground area for shrubs, trees, and total riparian vegetation.

ETa (mm/Year)	ETa (in/Year)	PP (in/Year)	WD (in/Year)	ETa (ft/Year)	WD (ft)	Area (Acres)	CU (Acre-ft)
Shrubs, West							
401.58	15.81	8.82	6.99	1.318	0.582	8995.10	5238.77
Trees, West							
573.95	22.60	9.50	13.10	1.883	1.091	99.40	108.50
West Subtotal							
403.67	15.89	8.83	7.06	1.324	0.589	9094.50	5353.02
Shrubs, East							
466.01	18.35	11.99	6.36	1.529	0.530	2811.26	1490.03
Trees, East							
515.43	20.29	10.09	10.20	1.691	0.850	385.30	327.47
East Subtotal							
472.09	18.59	11.75	6.83	1.549	0.569	3196.56	1820.08
Combined							
Full Area Shrubs							
414.74	16.33	9.47	6.86	1.361	0.572	11,806.36	6749.76
Full Area Trees							
530.28	20.88	9.94	10.93	1.740	0.911	484.70	441.67
ETa Navajo Nation Riparian ROI Total							
419.01	16.50	9.49	7.01	1.375	0.584	12,291.06	7181.55
ETo Navajo Nation Riparian ROI Total							
1488.27	58.59	9.49	49.11	4.883	4.092	12,291.06	50,299.61

Table 9 shows water metric estimates for the riparian ROI West–East division and the total study area within the Navajo Nation using coarser gridded input weather data from PRISM (4 km) and Landsat (30-m) to measure these metrics as the annual mean of seven years (2014–2020) using the rasterized 'best-approximation' method. Using the rasterized 'best-approximation' method with PRISM data, the West CU estimate is 31,760 AF and the East CU estimate is 10,317 AF. The combined total area (West and East) provided using CU estimated using the rasterized 'best-approximation' method with PRISM data is 41,585 AF. This method produced the highest values due to averaging all the input weather data within a 4 km × 4 km grid. The ETo is provided in the last row (shaded, blue). ETa is approximately 28% of the ETo. The CU based on ETa (41,585 AF) is approximately 16% of CU based on ETo (265,110 AF) (Table 9). Comparing results between the two rasterized 'best-approximation' methods, one using Daymet (1 km) (Table 7) and the other using PRISM (4 km) (Table 9), the finer resolution (Daymet) input CU data (36,983 AF) should be selected over the coarser resolution (PRISM) input data (41,585 AF). However, CU estimates using both raster-based methods with finer (Daymet) input data, including the 'conservative' estimate (31,648 AF) and the 'best-approximation' estimate (36,983 AF), and the coarser (PRISM) input data 'best-approximation' estimate (41,585 AF) all fall within the literature-reviewed estimated range of 25,387 AF to 46,397 AF. Therefore, our estimates from this study for CU, provided in Tables 6, 7 and 9, refine the literature-reviewed range produced prior to this research [32].

Table 9. Final water metric results for the riparian ROI showing the rasterized 'best-approximation' estimate of the mean data from 2014 to 2020 using gridded PRISM data (4 km) and Landsat (30-m) to derive ETa (mm, in, ft), PP (in), WD (in, ft) and ETo (mm, in, ft) (last row); the CU (acre-ft, last column) is calculated by ground area for shrubs, trees, and total riparian vegetation.

ETa (mm/Year)	ETa (in/Year)	PP (in/Year)	WD (in/Year)	ETa (ft/Year)	WD (ft/Year)	Area (Acres)	CU (Acre-ft)
Shrubs, West							
393.91	15.51	7.96	7.55	1.292	0.629	48,506.24	30,527.99
Trees, West							
560.87	22.08	7.34	14.75	1.840	1.229	594.24	730.19
West Subtotal							
395.93	15.59	7.64	7.52	1.299	0.637	49,100.48	31,760.35
Shrubs, East							
461.55	18.17	9.75	8.42	1.514	0.702	12,448.09	8735.84
Trees, East							
506.48	19.94	9.08	10.87	1.662	0.905	1746.91	1581.70
East Subtotal							
467.08	18.39	9.67	8.72	1.532	0.727	14,195.00	10,317.42
Combined							
Full Area Shrubs							
407.73	16.05	8.32	7.73	1.338	0.644	60,954.33	39,263.83
Full Area Trees							
520.29	20.48	8.63	11.85	1.707	0.988	2341.15	2311.89
ETa Navajo Nation Riparian ROI Total							
411.89	16.22	8.33	7.88	1.351	0.657	63,295.48	41,584.91
ETo Navajo Nation Riparian ROI Total							
1488.27	58.59	8.33	50.26	4.883	4.188	63,295.48	265,109.59

3.3. A Newer Nagler ET(EVI2) Method Based on Landsat and Gridded Weather Data from Daymet and PRISM for Riparian Corridor Water Use Estimation

Due to lack of ground-based weather station data in northeastern Arizona, we instead used gridded weather data to estimate water metrics (mm/year) for the Little Colorado River watershed riparian corridors. These water metrics include BC ETo, ETa, PP, and WD. ETa is estimated using Equations (4) and (5) which substitute gridded weather data and EVI2 into earlier formulations [55]. We provide these water metric estimates by riparian cover total and separately, shrubs versus trees, for each of the seven years (2014–2020), and the mean and standard deviation by shrub, trees and total riparian area for selected reaches within the Little Colorado River watershed.

Figure 6 shows an ETo map of the study area in northeast Arizona for one date in 2014 which ranges from an ETo of 1.5 (low) to 4 (high) mm/day. The region shows very high (red) ETo corresponding to the Little Colorado River mainstem and the Colorado River north of their convergence, with values above 3.2 mm/day. The area surrounding the city of Flagstaff in the southwest corner of Figure 6 have the lowest ETo, under 2 mm/day.

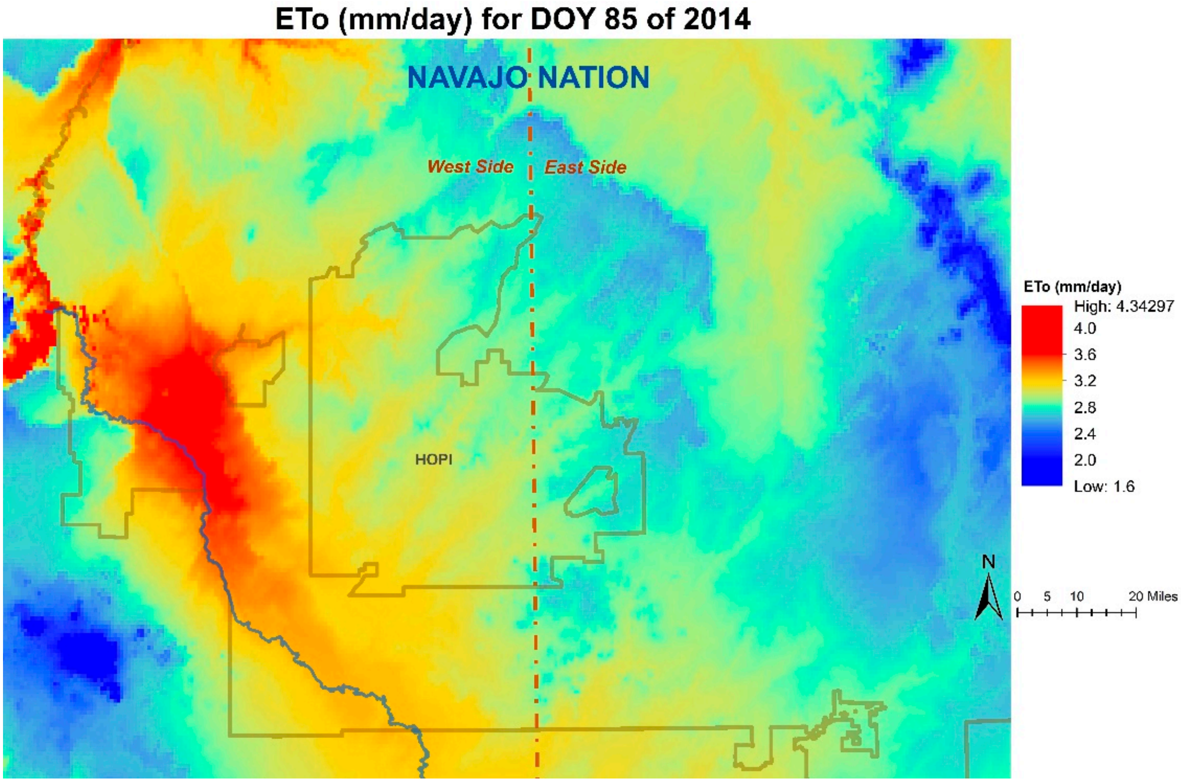

Figure 6. Map of potential evapotranspiration (ETo, mm/day) using Daymet (1 km resolution) for a single date (DOY 85) in 2014 for the northeast corner of Arizona which includes both the Hopi and Navajo Reservations and parts of the Little Colorado River watershed.

Using remote sensing based spatiotemporal data and analysis methods, we produced the first maps of the water metrics required to calculate CU for the riparian corridors along the Little Colorado River tributaries, streams, and springs. The method includes using meteorological data from Daymet (gridded 1 km) and PRISM (gridded 4 km), and a digitized product over high-resolution NAIP imagery, and finally Landsat-8/OLI imagery (30 m resolution, UTM, Zone 12) to produce maps of precipitation (PP, upper left), potential ET (ETo, upper right), actual ET (ETa, lower left) and the water requirement which is ETa-PP (WD, lower right) (Figure 7). The four panels are data averaged for one year (2017). The year 2017 was chosen as the data are similar to the average of the seven years of the study based on standard anomalies.

This study generated the first ETa map produced for this region, with data ranging from 100 to 900 mm/year, that covers both Hopi and Navajo Reservations for not only riparian corridors but also for the other land cover types. The plant water requirement or WD for the ROI is between 0–300 mm/year. ETo, or maximum plant water use, ranges between 800–2000 mm/year. Most of the lower elevation areas ranged in ETa between 100–500 mm/year, but were higher in mountains where measurements ranged between 600–800 mm/year (Figure 7).

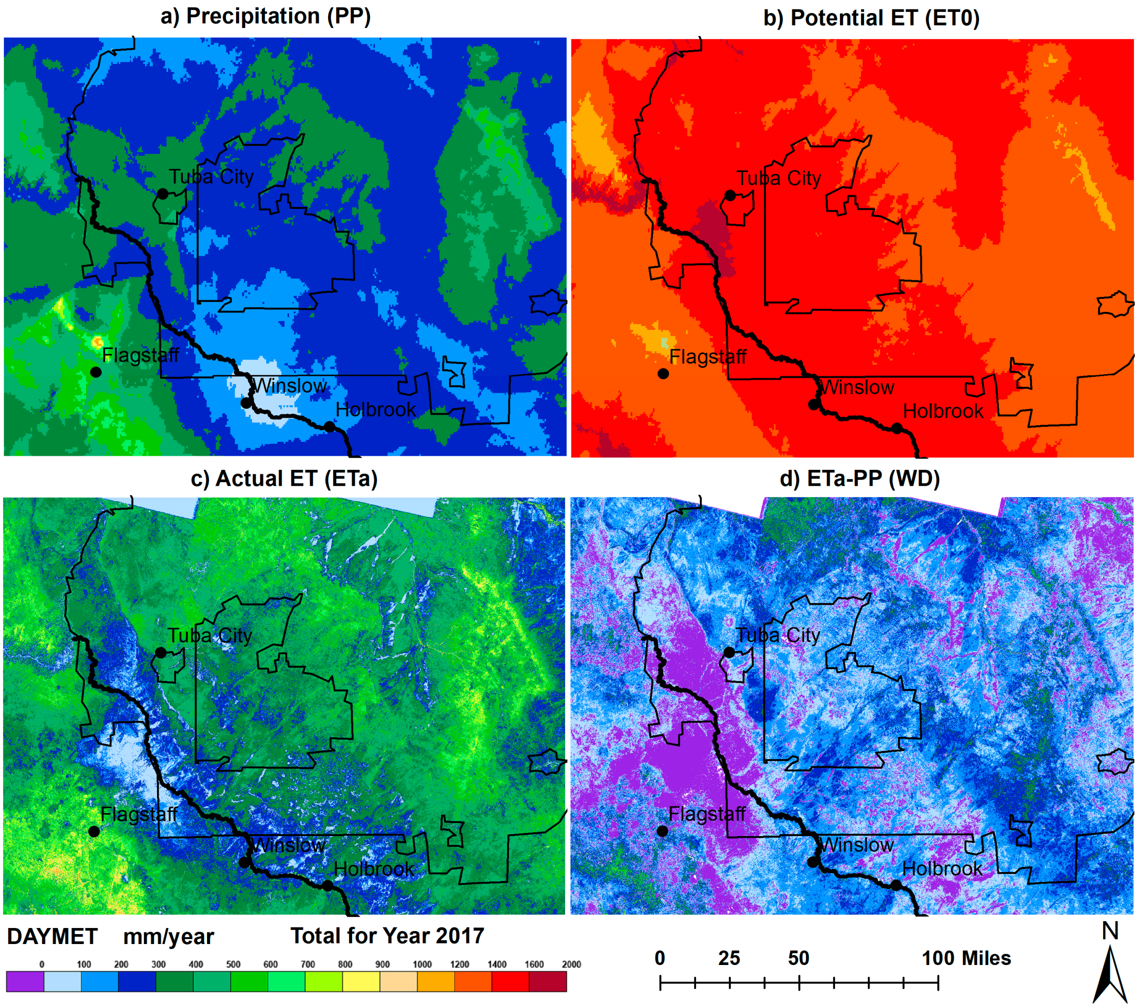

Figure 7. Annual water metrics ((**a**) precipitation (PP), (**b**) potential ET (ETo), (**c**) actual ET (ETa) and (**d**) net water requirement or ETa-PP (WD)) for 2017 using weather data from Daymet (gridded 1 km) and produced at Landsat 30 m resolution for northeast Arizona.

The set of four water metric maps were also produced using input from the coarse-resolution PRISM (4 km) weather data (Figure 8). Note that the ETa map (Figure 8c) follows the same spatiotemporal patterns as Figure 7c which used Daymet. The coarser resolution input data from PRISM helps to confirm the spatial range in ETa, as well as the other variables, because all the variables follow landcover features and vegetative classes.

The water metrics with Daymet (1 km) as the input weather data showing the mean values for ETo, ETa, PP, WD for the seven years (2014–2020) in this study are provided in a bar chart; their average is shown with the last bar on the right (Figure 9). The four metrics are shown separately for shrubs and trees (Figure 9a, top) and altogether for riparian vegetation (Figure 9b, bottom). These results show that ETo has remained stable across all years at approximately 1500 mm/year. There is a mostly positive and increasing trend in ETa and WD since 2015, and a generally decreasing trend in rainfall since 2015, as one would expect during these unprecedented times of drought, especially on the Colorado Plateau. ETa is highest in 2020, which was the year with the lowest rainfall; the opposite trends, i.e., the year 2015 with the highest PP had the lowest ETa, indicate more water is used by riparian vegetation when PP is limited. The year 2020 was drier (100 mm/year) than the other years 2015–2020, with 2014 having twice as much PP (200 m/year) as 2020 and 2015 twice the year before (2014) and the wettest at almost 400 mm/year.

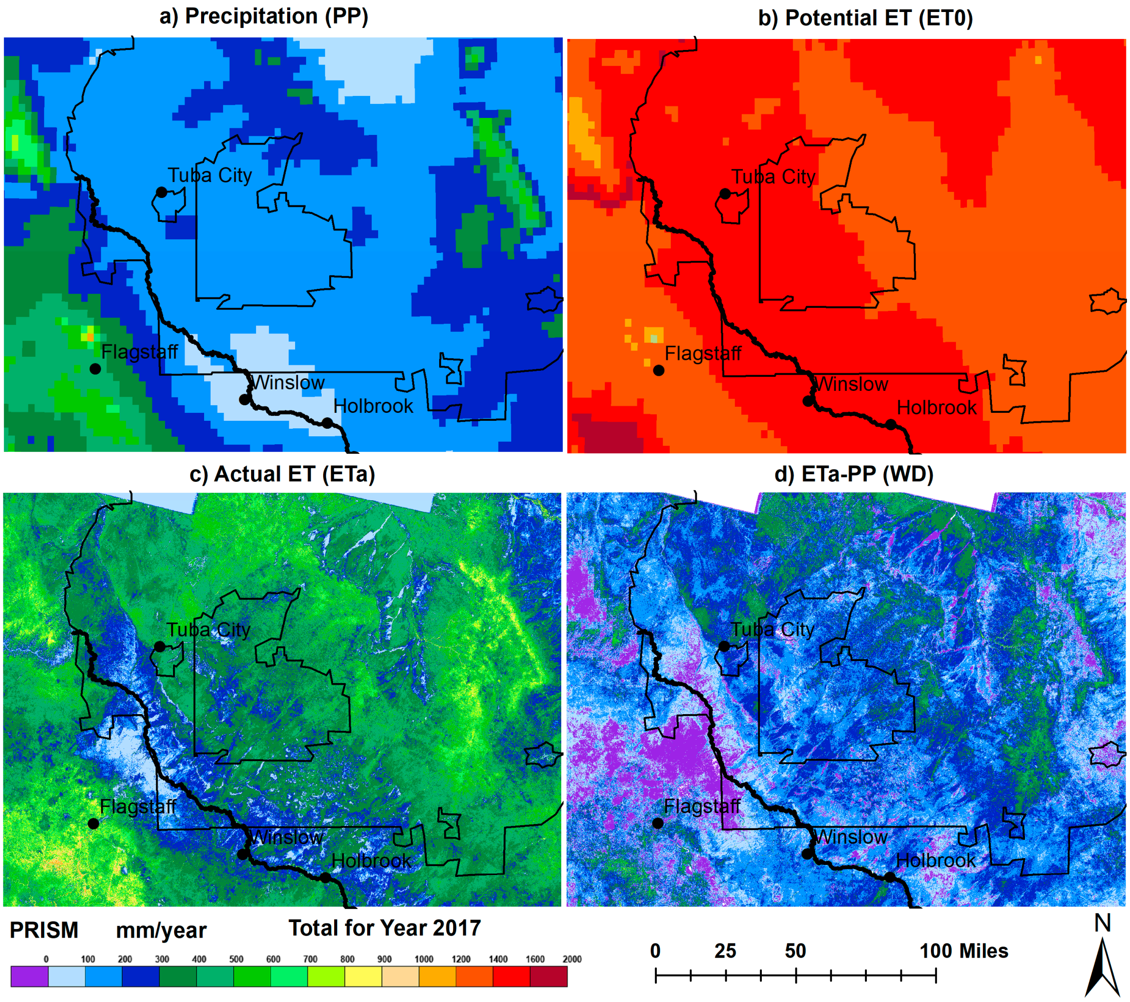

Figure 8. Annual water metrics [(**a**) precipitation (PP), (**b**) potential ET (ETo), (**c**) actual ET (ETa) and (**d**) net water requirement or ETa-PP (WD)] for 2017 using weather data from PRISM (gridded 4 km) and produced at Landsat 30 m resolution for northeast Arizona.

A line plot (Figure 10) shows the standardized anomalies of the measured water metrics (mm/year) estimated using Landsat imagery and Daymet for each of seven years (2014–2020) for the riparian corridor (combined shrubs and trees); the standard anomaly is calculated using the current value minus the average value and divided by the standard deviation. All four of the metrics are depicted: precipitation (PP), potential ET (ETo), actual ET (ETa), and the water deficit, ETa − PP (WD). While a short period of time to establish any trend, the plot shows an increase in ETa and WD from 2015 to 2020. The year 2015 was the wettest (ca. 400 mm/year) as depicted by its high anomaly (+>1.5) and the year 2020 was the driest with an anomaly of −1.5 (Figure 10). As expected, ETa and WD trends are similar and very close, following one another for all seven years. ETo in both 2014 and in 2020 are high anomalies (+1 and +1.5). Averaged over seven years, ETo for the 'best approximation' ROI is 259,029 AF; the 'best approximation' estimate of ETa using Daymet is estimated to be 419 mm/year (1.375 ft), while CU is 36,983 AF using Daymet.

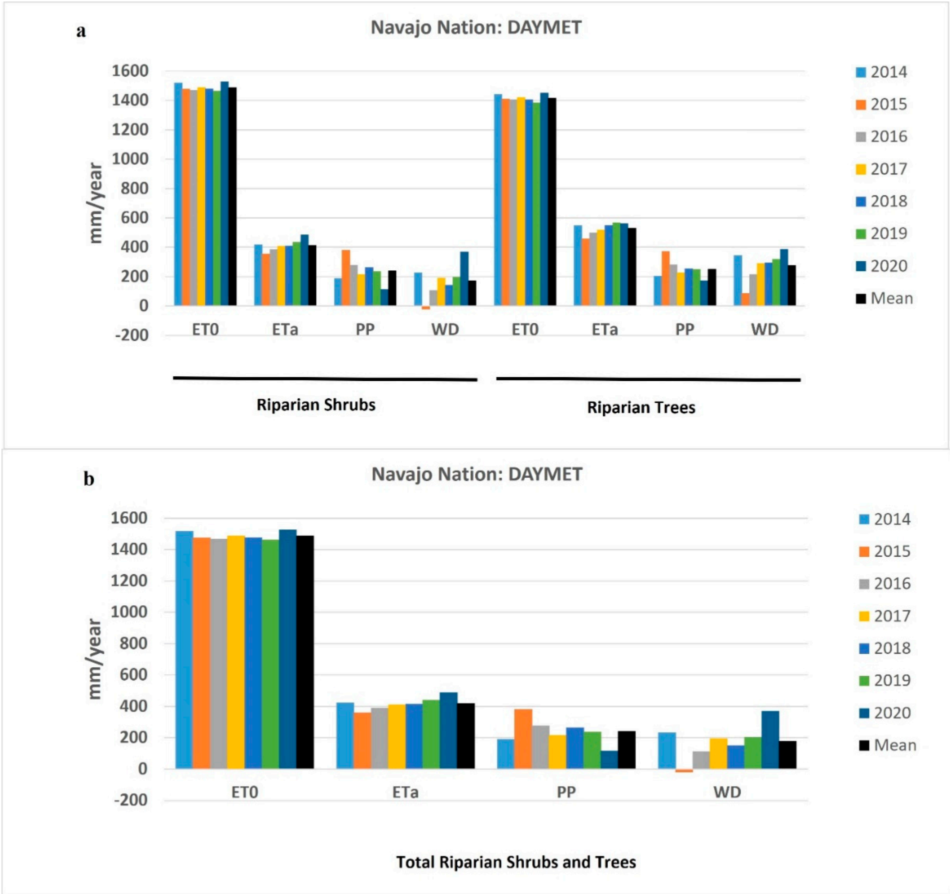

Figure 9. Summary bar plot showing the annual water balance (mm/year) estimated using 30 m resolution Landsat and weather variables from Daymet (gridded, 1 km) for each of the seven individual years (2014–2020), and their long-term average, for potential ET (ETo), actual ET (ETa), precipitation (PP), and the water deficit (WD) with results separated into shrubs and riparian trees ((**a**), top) and combined for total riparian vegetation ((**b**), bottom).

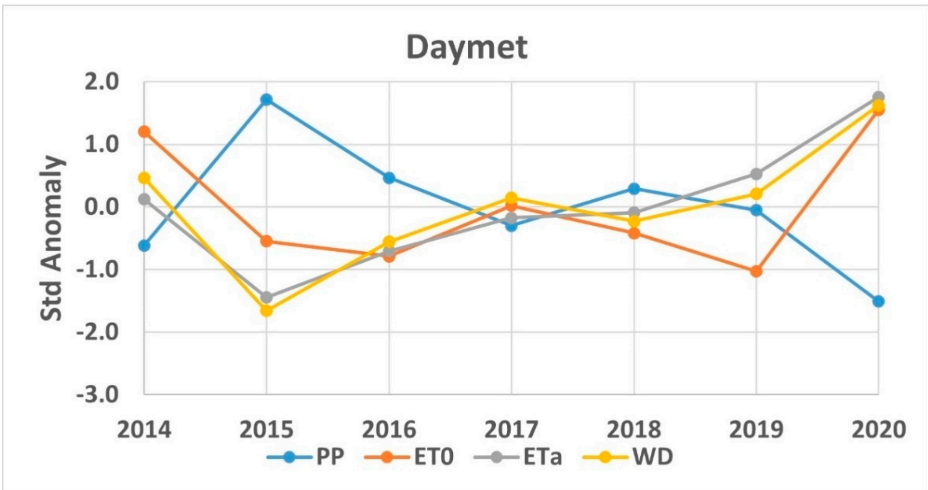

Figure 10. Standardized anomalies as line graphs of key water metrics, precipitation (PP), potential ET (ETo), actual ET (ETa), and water deficit (WD), for seven years (2014–2020) with weather data acquired using Daymet (gridded, 1 km) but produced at 30 m resolution for the northeast corner of Arizona, which includes a large portion of the Navajo Nation.

To determine if coarser resolution of the input meteorological data would have a significant impact on the water metric results, we also used PRISM (4 km) for all seven years to derive the average annual values for ETo, ETa, PP, and WD over the recent period (2014–2020) of the study; their average is shown with the last bar on the right (Figure 11). We provide the summary bar chart for comparison to Figure 9 which uses Daymet. The four metrics are shown separately for shrubs and trees (Figure 11a, top) and altogether for riparian vegetation (Figure 11b, bottom). These results show that ETo has remained stable across all years at approximately 1500 mm/year. There is a positive and increasing trend in ETa and WD, and a generally decreasing trend in rainfall over this short study period. Note that 2017 depicts the smallest, near zero, standard anomaly for all four water metrics. This is also the year from which we sourced the data in Figures 7 and 8.

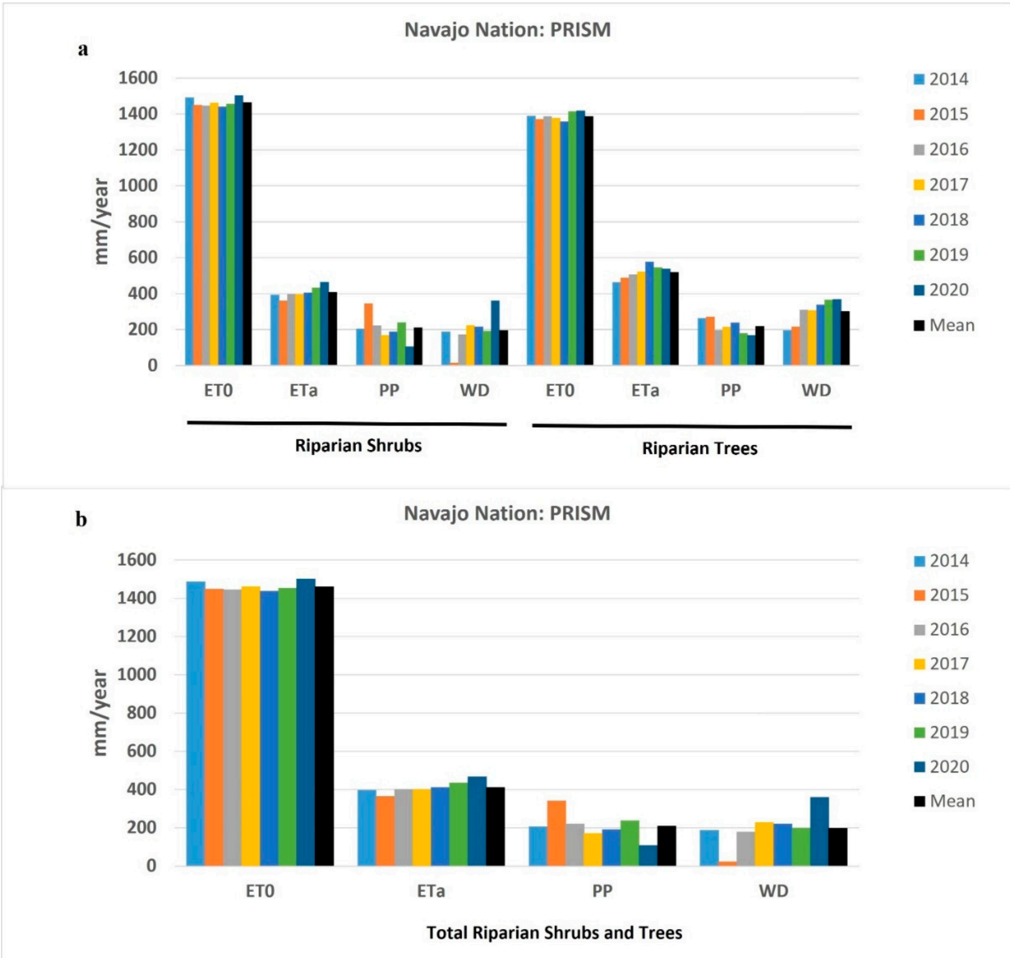

Figure 11. Summary bar plot showing the annual water balance (mm/year) estimated using 30 m resolution Landsat and weather variables from PRISM (gridded, 4 km) for each of the seven individual years (2014–2020), and their long-term average, for potential ET (ETo), actual ET (ETa), precipitation (PP), and the water deficit (WD) with results separated into shrubs and riparian trees ((**a**), top) and combined for total riparian vegetation ((**b**), bottom).

Another set of lines are plotted (Figure 12) to show the standardized anomalies of the water metrics (mm/year) estimated using Landsat imagery and PRISM for each of seven years (2014–2020) for the riparian corridor (combined shrubs and trees); the metrics are precipitation (PP), potential ET (ETo), actual ET (ETa), and the water deficit (WD) or ETa-PP. This figure provides the reader with a comparison of results between the use of Daymet (1 km) and PRISM (4 km). The standard anomaly trends for the water metrics are similar between these two scales. While still a short period of time to establish any trend, Figure 12 shows an increase in ETa and WD from 2015 to 2020 for PRISM as with Daymet

(Figure 10). The year 2020 was drier (100 mm/year) than the other years 2015–2020, with 2014 having twice as much PP (200 m/year) as 2020 and 2015 twice the year before (2014) and the wettest at ca. 375 mm/year using the coarser gridded dataset.

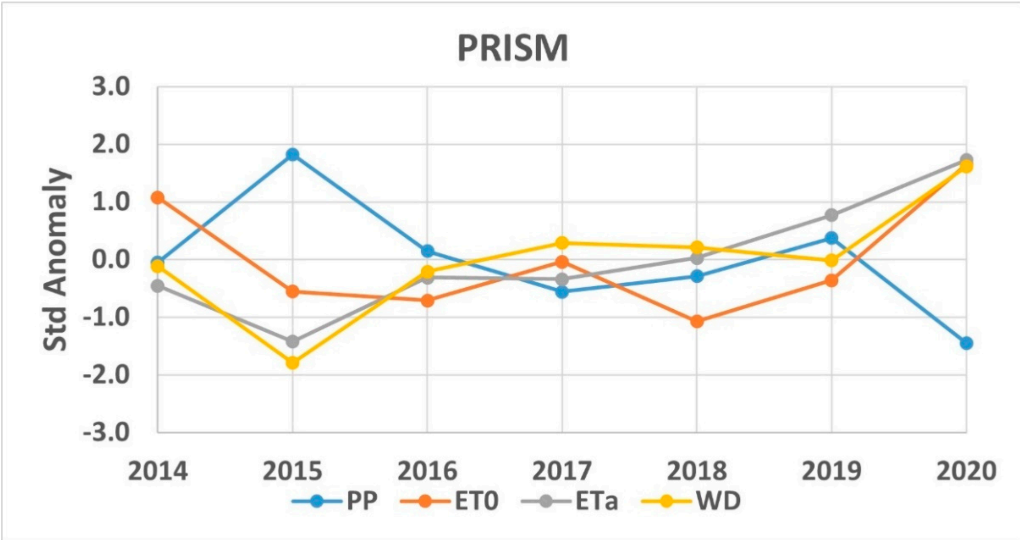

Figure 12. Standardized anomalies as line graphs of key water metrics, precipitation (PP), potential ET (ETo), actual ET (ETa), and water deficit (WD), for seven years (2014–2020) with weather data acquired using PRISM (gridded, 4 km) but produced at 30 m resolution for the northeast corner of Arizona, which includes a large portion of the Navajo Nation.

From Figure 12, we note that for PP, the year 2015 was wettest (ca. 375 mm/year) as depicted by its high anomaly (+1.9) and 2020 was the driest (100 mm/year) as seen by the low anomaly (−1.4). The year 2015 showed anomalies between −1 and −2 for ETa and WD, metrics which track each other. The year 2020 shows a high anomaly (+1.5) year for three of the metrics, ETo, ETa, and WD but shows a low anomaly (−1.5) for year 2020 (Figure 12). As with Figure 10, 2017 depicts the smallest, close to zero, standard anomaly for all four water metrics. All data figures and tables are provided through USGS Science Base [62].

4. Discussion

4.1. Vegetation Index-Based Evapotranspiration and Consumptive Use Estimation in the Literature

Using a VI-based equation, Nagler et al., 2020 showed ETa time series data for 20 years from 2000 to 2019 for the Lower Colorado River delta riparian zone [34]. The method was used to measure trend over time, for example, from 1130-mm/year (year 2000) to 654 mm/year (year 2019), demonstrating a decline on the order of ca. 35% over 20 years of 476 mm/year in this uniquely narrow landcover [34]. Similar losses were recorded on the U.S. portion of the Lower Colorado River [7].

Across different vegetation types and rainfall regimes, an inherent system sensitivity to available water was found such that there was similar ecosystem water-use efficiency regardless of hydroclimatic conditions [61]. Most ETa research focuses on cultivated landcover and overwhelmingly uses energy-balance ETa products that are now available across the U.S. in the form of the Simplified Surface Energy Balance operational (SSEBop) and SSEBop on Google Earth Engine [63]. For the western part of the U.S., there are a variety of thermal-based ET algorithms on Open ET [64] and there is Ecostress (on the Space Station) [65]. In Australia, there is the newly available CMRSET algorithm [66], and prior to this, other VI-based ETa estimation methods have been utilized [67,68]. VI-based ETa estimation has been used in dryland agricultural regions where crop coefficients are used for irrigation and precision crop management [69–72]. For vegetation communities dominant in riparian corridors, remote sensing has provided accurate, useful information on canopy attributes, thus making VI-based ETa a key method for plant water use estimation [73–75].

Jarchow et al., 2020 [76] produced estimates of ETa for a riparian river reach on the San Juan River in New Mexico and showed ETa ranged from 280 mm/year to 620 mm/year between 2000-2018. These values are slightly lower than other riparian corridors because the dominant riparian species, saltcedar, has been impacted by the leaf beetle, *Diorhabda* Spp. [77,78]. Although the presence of the defoliating beetle on the Colorado Plateau can be a great opportunity for riparian restoration [79], there is a lack of restoration on the tributaries of the Little Colorado River. Some monitoring work has been done in the restored and unrestored riparian areas of the Colorado River delta [80]. However, no outcomes have yet been determined there to quantify the biological control on water use in those riparian zones that contain saltcedar since the beetle has only recently been active as of 2021.

Because of the importance of phytoremediation of Legacy Mine sites on the Navajo Nation, several studies using ETa of native species have been conducted near Monument Valley [81,82]. On-the-ground measurements of plant water use, measured from sap flow sensors, produced estimates of transpiration of two main shrub species, *Atriplex canescens* and *Sarcobatus vermiculatus* [81]. The water use measured by sap flux measurements in the dryland phreatophyte shrub communities on the Navajo Nation were scaled to MODIS using EVI [82]. In the same time frame, other studies were scaling from sap flux to the wider riparian reach with remote sensing technology being developed using scaled EVI (EVI*) from MODIS. This method was used to scale ETa over agricultural and riparian areas along the Lower Colorado River in the arid southwestern US [30,31] following Groeneveld's NDVI* process [83]. In the first application of this scaling method on the Navajo Nation, transpiration was projected over the area for a site of 318 ha near Comb Ridge and for these species, they measured 1.54 mm/day and ranging between 1.0 mm/day to 1.9 mm/day. This range is between 73 mm/year and 163 mm/year for years 2000–2007 [81]. Bresloff et al., 2013 [82] then used EVI * to derive ETa for the phreatophyte shrub communities at the same site in Monument Valley on the Navajo Nation. They reported results showing ETo, PP (mm/year), and ETa in mm/year for three plots in the years 2000–2010. The study reported the mean ET of 137 mm/year for years 2000–2004 and 186 mm/year for years 2005–2010 [82]. Mean PP varied from 139 mm/year to 166 mm/year during the study period (2000–2010), ETo ranged between 1504 mm/year (2000–2004) and 1442 mm/year (2005–2010), and the peak ETa of native species, observed in July, ranged between 1.18 mm/day and 1.52 mm/day [82]. Values of ETa over ten years ranged from 75 mm/year in 2002 to 240 mm/year in 2010 [82]. These estimates of ETo, ETa and PP from these two studies [81,82] were later used to construct a water balance of the Legacy Mine site in Tuba City, Arizona, on the Navajo Nation using the same ETa estimation method [84]. Jarchow et al., 2020 also modified the Groeneveld equation [83] and used a scaled NDVI (NDVI *) to calculate vegetation health and ETa dynamics for non-native saltcedar (*Tamarisk* spp.) along the floodplain on the Navajo Nation near Shiprock, New Mexico [84]. In other non-riparian vegetation community research, they measured ETa in a semiarid sagebrush steppe where ETa was calibrated with a 3-ha lysimeter [85].

The values from these studies are summarized for ETo, ETa, PP and WD in Table 3 for comparison with other riparian or phreatophyte plant community studies' findings that report on water metric means [30,31,45,81,82]. The reported values from the literature are very close to the values we report in this study which use slightly revised ETa methods that include gridded weather data and EVI2 from Landsat-8/OLI. Input weather data for the Navajo Nation are lacking and therefore we improvised by using the BC ETo from gridded sources. The primary reason for doing so is that BC is quite simple in that it only requires a direct measurement of temperature and precipitation [20,21,52,53]. Other research that utilizes BC over the PM ETo estimation in this region is provided in more detail [76,85], but the main reason is that it requires many climatic parameters and incorporates physiological and aerodynamic data that are typically measured in crop studies [21,76]; this study of arid natural riparian zones is not suited for using this level of detail. Jarchow et al., 2020 found a comparison of these two methods specifically for studies in arid environments. The differences between PM and BC range from <1% to >30%, with BC commonly overestimating ETo with respect to PM [76,85,86]. Although PM is typically more accurate in measuring ETa, there are many sites where measurement of the long list of input variables jointly with the difficulty in acquiring and ascertaining their mean values deems this method to be unrealistic. Therefore, like many studies conducted on the Navajo Nation, we solely use BC for ETo.

The Arizona Department of Water Resources (ADWR) mapped 13,457 acres of riparian vegetation along streams on the Hopi Reservation [43]. Based on this acreage, an estimated total annual water demand of 2.3 to 4.4 AF was determined based on previous research of riparian water use along the Rio Grande in NM [87]. Compared with Table 3 in this study, our literature review [32] had an expected range of 1.74 to 3.75 AF and PP of 5–6 in. The ADWR 2008 report [43] summarized PP from 2005 to be in the range of 0.5 AF to 0.7 AF. The conclusion from the Hopi Preliminary Hydrographic Survey Report Tables 8 and 9 (2008) was that the CU ranged between 23,134 to 56,390 AF for this area of riparian vegetation [43]. We highlight these additional key findings that produced estimates within the range of CU of our study. Their important estimates of water use were not included in the original literature review [32] because of a lack of access at that time. We now add their range of CU to our discussion because their median estimate of CU of 39,762 AF in 2008 is remarkably close to our findings using the mean (36,739 AF) of our three methods; their study very much supports our range of estimates between Daymet and PRISM resolutions (31,648 to 41,585 AF) and complements our study.

4.2. Riparian Vegetation Consumptive Use by Area

There are limitations to the quantification of all riparian vegetation using these rasterization methods. The buffered methods still leave out vegetation that should be included for a more accurate estimate of vegetative cover. Therefore, vegetation cover estimates could be improved if more resources were put into perfecting the hand-digitization. In a previous study using MODIS pixels at 250 m spatial resolution to compute groundwater-discharge-by-vegetation, the gridded cells were downsampled to 50 m using nearest-neighbor interpolation for further analyses. Tillman et al., 2012 used these gridded values that were spatially associated with the combined stream buffer and land cover areas to include in their summary statistics for their study to estimate basin-scale groundwater discharge by vegetation in Arizona [88]. The study focused on the southern portion of Arizona [88]. In this basin and range province of Arizona study, they also used Blaney-Criddle with PRISM data; however, our study is the first to apply the ETa method using ETo from Blaney-Criddle using PRISM data explicitly to riparian corridors.

We produced three estimates of riparian vegetation area. The 'conservative' raster-area estimate was 19,362 ha (47,846 acres) and the 'best-approximation' raster-area for the riparian corridor was 25,615 ha (63,296 acres), whereas the digitized area included only a fraction of the total vegetative area, was only 4974 ha (12,291 acres).

We produced three estimates of CU based on these riparian area measurements: one from the digitized vector area, a second from the 'conservative' estimate from the rasterized area, and a third from the 'best-approximation' estimate from the rasterization, which captured the most riparian vegetation. The combined total area (merged West and East) of the Navajo Nation had a CU 'conservative' estimate using Daymet and Landsat of 31,648 AF (Table 6), a 'best-approximation' estimate using Daymet and Landsat of 36,983 AF (Table 7) in comparison with the lowest estimate using digitized polygons from NAIP and Daymet of 7,182 AF (Table 8). The rasterized 'best-approximation' CU estimate using the coarser weather data from PRISM and Landsat is 41,585 AF (Table 9).

Note that using two different scales for the weather variables results in very close estimates of ETa. The 'best-approximation' rasterization methods only have a measured difference of 7 mm/year; the values are 419 mm/year by Daymet and 412 mm/year by PRISM. Importantly, the vector-based method of 'digitized polygons' and the rasterized 'best-approximation' have exactly the same values for ETa, PP, ETo, but differ only in their area and thus their CU (Tables 7 and 8). The reason that ETa may have a lower value, but have a higher CU value (compare Table 6 to Table 7) is because the rasterizing method may include more riparian pixel area, however those pixels may contain more bare soil and result in a lower ETa value, such as in Table 6 for the 'conservative' estimates of CU. These results have now been compared to a 2020 dissertation focused on the same region which includes both the Navajo and Hopi Reservations [89]. In Section 3 of this work, ETa by season was found to be primarily under 110 mm / season with the higher ETa values (>60 mm) in the East. In Section 4, seasonal precipitation-evapotranspiration-consumption maps in tons/season are presented for the Navajo Nation on a $0.1^{o} \times 0.1^{o}$ grid. These results agree with our assessment that a West–East division exists based on the physiographics and that the East has a greater water deficit at peak season [89].

The 'best approximation' estimates for CU between the two input sources ranged from 36,983 AF (Daymet) to 41,585 AF (PRISM), a difference of 4602 AF. The median estimate using three of the rasterized methods is 36,739 AF, 244 AF less than the 36,983 AF 'best-approximation' estimate using Daymet and Landsat. Both the CU median value of 36,739 AF and the mean value of the Daymet 'best approximation' of 36,983 AF are nearly the same as reported in 2008 for the Hopi Reservation's median estimate of riparian CU (39,762 AF) [43] and 1823 AF less than what we report in this study using the 'best-approximation' CU estimate of 41,585 AF from PRISM and Landsat. For the purposes of this study, we show values from the two resolutions, but we suggest using Daymet with its higher 1 km resolution and the 'best-approximation' raster method, which includes more pixels over the riparian corridor, and produces a solid and reliable CU estimate of 36,983 AF. Our method produces a value that is 2779 AF short of the median value of 39,762 AF from the range of 23,134 AF to 56,390 AF that was provided in the Preliminary Hydrographic Survey Report for the Hopi Reservation (Preliminary HSR, Tables 8 and 9) [43].

4.3. Quantification of Percent Changes for Ranges of Years

The objectives of this study were to produce values for the water metrics, ETo, ETa, PP, and WD, and using the given riparian ROI area, quantify CU for one year. Because of the Landsat-8/OLI record, we instead provide these metrics for seven years, annually, and report the water metric averages for this 2014–2020 period. The bar plots in Figure 9 (with input Daymet weather data) and Figure 11 (with input PRISM weather data) show that 2020 was higher than other years in ETo, ETa and WD and that PP was higher in 2015 than all other years. Furthermore, these bars show that 2015 had the lowest ETa and WD and these two metrics track each other at both resolutions of Daymet and PRISM. Because of these two anomaly years of 2015 and 2020, we quantify the percent change for four sets of years: (i) 2014–2020, (ii) 2014–2019, (iii) 2015–2020, and (iv) 2015–2019. Using the values in Table 5 from the 'best-approximation' raster method with the higher resolution input weather data from Daymet, we summarize percent change for these sets of years so that the variability within selected ranges can be assessed.

We address (i) by including all seven years in this study, 2014 through 2020. The average annual ETa (mm/year) increased from 423.9 mm/year to 489.2 to mm/year or 65.3 mm/year (15%) over the recent seven years, 2014–2020. Precipitation decreased by 73.1-mm/year (a decrease of 38%) from 190.8 mm/year (2014) to 117.7 mm/year (2020). The water requirement/demand or deficit (WD), like ETa, shows an increasing trend from 233.1 mm/year (2014) to 371.5 mm/year (2020); this is an increase in WD of 138.4 mm/year (59%). The year 2015 had sufficient PP such that WD was negative 19.7 mm/year.

We address (ii) by excluding 2020, and report the percent changes over 2014–2019. The average annual ETa (mm/year) increased from 423.9 mm/year to 440.2 to mm/year or 16.3 mm/year (4%) over the recent six years, 2014–2019. Precipitation decreased by 46 mm/year (24%) from 190.8 mm/year (2014) to 236.8 mm/year (2019). The water requirement/demand or deficit (WD), shows a decreasing trend from 233.1 mm/year (2014) to 203.4 mm/year (2019); this is an decrease in WD of 29.7 mm/year (a decrease of 13%).

We address (iii) by excluding 2014, and report the percent changes over 2015–2020. The average annual ETa (mm/year) increased from 361.3 to 489.2 mm/year or 127.9 mm/year (35%) over the recent six years, 2015-2020. Precipitation decreased by 263.2 mm/year (a decrease of 69%) from 380.9 mm/year (2015) to 117.7 mm/year (2020). The water requirement/demand or deficit (WD), like ETa, shows an increasing trend from -19.7 mm/year (2015) to 371.5 mm/year (2020); this is an increase in WD of 391.2 mm/year.

We address (iv) by excluding 2014 and 2020 and report on the percent change between the years 2015–2019. The average annual ETa (mm/year) increased from 361.3 mm/year to 440.2 mm/year or 78.9 mm/year (22%) over the middle five years of the study, 2015–2019. Precipitation decreased by 144.1-mm/year (a decrease of 38%) from 380.9 mm/year (2015) to 236.8 mm/year (2019). The water requirement/demand or deficit (WD), like ETa, shows an increasing trend from −19.7 mm/year (2015) to 203.4 mm/year (2019); this is an increase in WD of 223.1 mm/year.

4.4. Limitations

The use of Landsat-8/OLI imagery in time-series for quantifying riparian corridor ETa using existing VI-based plant water use estimates has been validated with sap flow and eddy covariance methods, and even lysimeter methods, for the specific plant types or vegetation communities that exist along the streams on the Navajo Nation. However, this study did not acquire any comparison ground-based water use data. The newer Nagler ET(EVI2) algorithm [34] used in this study is specifically for use in riparian corridors in arid and semi-arid landscapes. This study used gridded weather data for the first time, replacing ETo estimates previously acquired from ground-based weather station data. Prior to this study, we had not implemented this ETa algorithm or the new method of using Daymet and PRISM. We do use these two meteorological data models, Daymet and PRISM, to develop observations where there are currently no measurements. These data are only as good as the underlying field data that the models are based on and in our case study, the accuracy of our gridded meteorology data could not be validated due to a lack of measurements in this region. Therefore, we only have comparison data using a paucity of ground data available from the Navajo and Hopi Reservations, and from other regions, such as from the Lower Colorado River where we utilized point-based ground measurements. Therefore, we have two main limitations: (1) we use ETa methods that may misrepresent the evaporative component of ET, and (2) we have limited on-site measurements and must rely on gridded data, which could lead to uncertainty in our estimates. The uncertainty is likely biased to more arid conditions given the small riparian area within the provided gridded data of 1- or 4 km pixels. We should note for the reader that (1) evaporation is almost negligible because there is very low precipitation and the groundwater is deep enough to only be transpired through plant uptake, (2) ET estimates include combined components of evaporation and transpiration because the areal resolution of the satellite imagery forces sub-pixel vegetation heterogeneity in estimates of ET, and (3) runoff is excluded, as well as other variables typically included in water balance, for this study on the Navajo Nation; however, our estimates will be improved in the future when we get more ground-based observations. Our reported net water requirement or water demand (WD) values are even less than those reported in the literature for riparian corridors in Table 3, values which are likely to be the "lower limit" because runoff, evaporation and rainfall were low or not considered in the estimation of the WD. In our measurements in this study, the WD is primarily based on riparian shrubs and not trees and the literature values in Table 3 came from more dense riparian corridors than those in this ROI. There are two important reports on the feasibility of developing large area ETa networks that should be considered when evaluating our findings against these reported data from research in Texas [90,91].

Another important caveat of this study is that we report our findings based on just the seven years that OLI data was initially collected, and we have not made comparisons using the new Landsat 9 imagery. On the other hand, Nagler et al., 2022 recently made comparisons between ETa estimation methods using Landsat-8/OLI [92]. In this study of the Lower Colorado River riparian corridor [92], we compared ETa between ET(EVI2) and SSEBop energy-balance and found that since the year 2000, ET(EVI2) decreased by 22% (286.12 mm/year) while SSEBop decreased 14% (116.96 mm/year) [92]. Comparing ET(EVI2) and ET(SSEBop) we found a difference of 260.62 mm/year over the recent five-year averaged period with ET(EVI2) equal to 996.30 mm/year and SSEBop equal to 735.69 mm/year, which may be explained in part by the 100 m thermal band used in SSEBop [92]. For this study of the riparian vegetation along the Little Colorado River tributaries, streams, and springs, we can make an educated guess based on the comparison work in the previously described study [92] that SSEBop estimates of ETa would be lower than our methods using ET(EVI2) because of the coarse thermal band utilized in the remotely sensed energy balance methods.

5. Conclusions

Our remotely sensed measurements of CU for the total riparian ROI, which is the vegetated corridor of the Little Colorado River tributaries, streams and springs, range from 31,648 AF ('conservative') to 36,983 AF ('best-approximation'; Daymet) to 41,585 AF ('best-approximation'; PRISM). The discrepancy between the latter two estimates is due only to the resolution between Daymet and PRISM weather data. Prior to this research, we used literature-based values from studies of uncultivated plant water use in the U.S. Southwest published between 2005–2020, which are summarized in Table 3, to estimate a range of CU values based on the expected riparian vegetation cover for the Little Colorado on the Navajo Nation, which was comprised mainly of shrubs with a few trees.

The range in water requirement/demand or deficit (WD) using published literature between 2005–2020 ranged between 20.87 in (1.74 ft) and 38.14 in (3.18 ft). Based on these values and the area of 14,598 acres for the riparian vegetation we previously projected CU to be between 25,387 AF and 46,397 AF [32].

Using the new, direct estimates in this remote sensing study, we calculate a 'conservative' estimate of the water deficit (WD) to be 7.94 in/year or 0.66 ft and ETo to be 4.1 ft/year; the ETa for riparian vegetation along the Little Colorado River tributaries and streams was estimated to be 17.29 in/year or 1.44 ft/year. The 'conservative' estimate of CU is 31,648 AF.

Our 'best-approximation' estimate of the water deficit (WD) is 7.01 in/year or 0.58 ft and ETo to be 4.1 ft/year; the ETa for riparian vegetation along the Little Colorado River tributaries, streams and springs was estimated to be 16.5 in/year or 1.38 ft/year. The 'best-approximation' estimate of CU is 36,983 AF.

These CU findings for riparian ecosystems along the Little Colorado River range between 31,648 AF and 36,983 AF and improve earlier estimates by narrowing the range of CU originally reported in the literature between 25,387 AF to 46,397 AF using data from similar ecosystems. This study provides better estimates of water use that will be valuable to the Navajo Nation and will assist with decision-making by natural resource managers and water resources planners tasked with managing habitat and water resources along these riparian corridors.

Author Contributions: Conceptualization, P.L.N. and K.D.; methodology, P.L.N., A.B.-M. and K.D.; software, A.B.-M., I.S. and K.D.; validation, A.B.-M., I.S. and K.D.; formal analysis, P.L.N., A.B.-M. and I.S.; investigation, P.L.N.; resources, A.B.-M. and K.D.; data curation, A.B.-M., I.S. and K.D.; writing—original draft preparation, P.L.N.; writing—review and editing, P.L.N., I.S., M.R.L. and K.D.; visualization, A.B.-M. and I.S.; supervision, P.L.N.; project administration, K.D.; funding acquisition, P.L.N. All authors have read and agreed to the published version of the manuscript.

Funding: This research was funded by U.S. Geological Survey and the University of Arizona, grant number G18AC00321-04.

Institutional Review Board Statement: Not applicable.

Informed Consent Statement: Not applicable.

Data Availability Statement: Data generated during this study are available from the USGS ScienceBase-Catalog (Nagler et al., 2022) [61].

Acknowledgments: We are grateful to Fred Phillips Consulting and the Navajo Nation for bringing these research questions to the U.S. Geological Survey. We wish to thank four reviewers from the U.S. Government who provided thorough and constructive reviews: Kul Khand (USGS, EROS), Pradeep Wagle (USDA, ARS), Fred Tillman (USGS, AZWSC), and Todd Caldwell (USGS, NVWSC). Any use of trade, firm, or product names is for descriptive purposes only and does not imply endorsement by the U.S. Government.

Conflicts of Interest: The authors declare no conflict of interest. The funders had no role in the design of the study; in the collection, analyses, or interpretation of data; in the writing of the manuscript, or in the decision to publish the results.

References

1. Ffolliott, P.F.; Baker, M.B., Jr.; DeBano, L.F.; Neary, D.G. Introduction. In *Riparian Areas of the Southwestern United States: Hydrology, Ecology and Management*; Baker, M.B., Jr., Ffolliott, P.F., DeBano, L.F., Neary, D.G., Eds.; CRC Press: Boca Raton, FL, USA, 2004; pp. 1–9.
2. Zaimes, G.; Nichols, M.; Green, D.; Crimmins, M. Defining Arizona's Riparian Areas and their Importance to the Landscape, Characterization of Riparian Areas, Hydrologic and Stream Processes in Riparian Areas. In *Understanding Arizona's Riparian Areas*; College of Agriculture and Life Sciences, University of Arizona: Tucson, AZ, USA, 2007; pp. 1–54. Available online: https://repository.arizona.edu/handle/10150/146921 (accessed on 12 December 2022).
3. Rood, S.B.; Goater, L.A.; Mahoney, J.M.; Pearce, C.M.; Smith, D.G. Floods, fire, and ice: Disturbance ecology of riparian cottonwoods. *Botany* **2007**, *85*, 1019–1032.
4. Loheide, S.P.; Booth, E.G. Effects of changing channel morphology on vegetation, groundwater, and soil moisture regimes in groundwater-dependent ecosystems. *Geomorphology* **2011**, *126*, 364–376. [CrossRef]
5. Nagler, P.L.; Pearlstein, S.; Glenn, E.P.; Brown, T.B.; Bateman, H.L.; Bean, D.W.; Hultine, K.R. Rapid dispersal of saltcedar (Tamarix spp.) biocontrol beetles (*Diorhabda carinulata*) on a desert river detected by phenocams, MODIS imagery and ground observations. *Remote Sens. Environ.* **2014**, *140*, 206–219. [CrossRef]
6. Singh, R.K.; Senay, G.B.; Velpuri, N.M.; Bohms, S.; Scott, R.L.; Verdin, J.P. Actual Evapotranspiration (Water Use) Assessment of the Colorado River Basin at the Landsat Resolution Using the Operational Simplified Surface Energy Balance Model. *Remote Sens.* **2014**, *6*, 233–256. [CrossRef]
7. Nagler, P.L.; Barreto-Muñoz, A.; Chavoshi Borujeni, S.; Nouri, H.; Jarchow, C.J.; Didan, K. Riparian area changes in greenness and water use on the Lower Colorado River in the USA from 2000–2020. *Remote Sens.* **2021**, *13*, 1332. [CrossRef]
8. Loheide II, S.P.; Gorelick, S.M. A local-scale, high-resolution evapotranspiration mapping algorithm (ETMA) with hydroecological applications at riparian meadow restoration sites. *Remote Sens. Environ.* **2005**, *98*, 182–200. [CrossRef]
9. Yang, H.; Rood, S.B.; Flanagan, L.B. Controls on ecosystem water-use and water-use efficiency: Insights from a comparison between grassland and riparian forest in the northern Great Plains. *Agric. For. Meteorol.* **2019**, *271*, 22–32. [CrossRef]
10. Loheide, S.P.; Gorelick, S.M. Riparian hydroecology: A coupled model of the observed interactions between groundwater flow and meadow vegetation patterning. *Water Resour. Res.* **2007**, *43*, W07414. [CrossRef]
11. Flanagan, L.B.; Orchard, T.E.; Logie, G.S.; Coburn, C.A.; Rood, S.B. Water use in a riparian cottonwood ecosystem: Eddy covariance measurements and scaling along a river corridor. *Agric. For. Meteorol.* **2017**, *232*, 332–348. [CrossRef]
12. Flanagan, L.B.; Orchard, T.E.; Tremel, T.N.; Rood, S.B. Using stable isotopes to quantify water sources for trees and shrubs in a riparian cottonwood ecosystem in flood and drought years. *Hydrol. Process.* **2019**, *33*, 3070–3083. [CrossRef]
13. Lurtz, M.R.; Morrison, R.R.; Gates, T.K.; Senay, G.B.; Bhaskar, A.S.; Ketchum, D.G. Relationships between riparian evapotranspiration and groundwater depth along a semiarid irrigated river valley. *Hydrol. Process.* **2020**, *34*, 1714–1727. [CrossRef]
14. Breshears, D.D.; Myers, O.B.; Meyer, C.F.; Barnes, F.J.; Zou, C.B.; Allen, C.D.; McDowell, N.G.; Pockman, W.T. Tree die-off in response to global change-type drought: Mortality insights from a decade of plant water potential measurements. *Front. Ecol. Environ.* **2009**, *7*, 185–189. [CrossRef]
15. Seager, R.; Ting, M.; Held, I.; Kushnir, Y.; Lu, J.; Vecchi, G.; Huang, H.P.; Harnik, N.; Leetmaa, A.; Lau, N.C.; et al. Model projections of an imminent transition to a more arid climate in southwestern North America. *Science* **2007**, *316*, 1181–1184. [CrossRef] [PubMed]
16. Stevens, L.E.; Meretsky, V.J. *Aridland Springs in North America Ecology and Conservation*; University of Arizona Press and The Arizona-Sonora Desert Museum: Tucson, AZ, USA, 2008; p. 432.
17. Stevens, L.E.; Jenness, J.; Ledbetter, J.D. Springs and Springs-Dependent Taxa of the Colorado River Basin, Southwestern North America: Geography, Ecology and Human Impacts. *Water* **2020**, *12*, 1501. [CrossRef]
18. Gribovszki, Z.; Kalicz, P.; Szilagyi, J.; Kucsara, M. Riparian zone evapotranspiration estimation from diurnal groundwater level fluctuations. *J. Hydrol.* **2008**, *349*, 6–17. [CrossRef]
19. Khand, K.; Taghvaeian, S.; Hassan-Esfahani, L. Mapping annual riparian water use based on single-satellite-scene approach. *Remote Sens.* **2017**, *9*, 832. [CrossRef]

20. Jensen, M.E.; Burman, R.D.; Allen, R.G. Evapotranspiration and Irrigation Water Requirements. In *ASCE Manuals and Reports on Engineering Practice No. 70*; American Society of Civil Engineers (ASCE): New York, NY, USA, 1990.
21. Allen, R.; Pereira, L.; Rais, D.; Smith, M. *Crop Evapotranspiration—Guidelines for Computing Crop Water Requirements—FAO Irrigation and Drainage Paper 56*; Food and Agriculture Organization of the United Nations: Rome, Italy, 1998.
22. Nagler, P.; Scott, R.; Westenburg, C.; Cleverly, J.; Glenn, E.; Huete, A. Evapotranspiration on western U.S. rivers estimated using the Enhanced Vegetation Index from MODIS and data from eddy covariance and Bowen ratio flux towers. *Remote Sens. Environ.* **2005**, *97*, 337–351. [CrossRef]
23. Nagler, P.L.; Glenn, E.P.; Kim, H.; Emmerich, W.; Scott, R.L.; Huxmam, T.E.; Huete, A.R. Relationship between evapotranspiration and precipitation pulses in a semiarid rangeland estimated by moisture flux towers and MODIS vegetation indices. *J. Arid Environ.* **2007**, *70*, 443–462. [CrossRef]
24. Nagler, P.; Jetton, A.; Fleming, J.; Didan, K.; Glenn, E.; Erker, J.; Morino, K.; Milliken, J.; Gloss, S. Evapotranspiration in a cottonwood (*Populus fremontii*) restoration plantation estimated by sap flow and remote sensing methods. *Agric. For. Meteoro.* **2007**, *144*, 95–110. [CrossRef]
25. Nagler, P.L.; Morino, K.; Didan, K.; Osterberg, J.; Hultine, K.; Glenn, E. Wide-area estimates of saltcedar (*Tamarix* spp.) evapotranspiration on the lower Colorado River measured by heat balance and remote sensing methods. *Ecohydrology* **2009**, *2*, 18–33. [CrossRef]
26. Jensen, M.E. *Coefficients for Vegetative Evapotranspiration and Open Water Evaporation for the Lower Colorado River Accounting System*; United States Bureau of Reclamation, Boulder Canyon Operations Office: Boulder City, NV, USA, 1998.
27. USBR, United States Bureau of Reclamation; LCRAS, Lower Colorado River Accounting System. *Evapotranspiration and Evaporation Calculations, Calendar Year 2007*; United States Bureau of Reclamation: Boulder City, NV, USA, 2008.
28. Nagler, P.; Glenn, E.P.; Hursh KCurtis, C. Vegetation Mapping for Change Detection on an Arid-Zone River. *Environ Monit Assess.* **2005**, *109*, 255–274. [CrossRef] [PubMed]
29. Nagler, P.L.; Glenn, E.P.; Hinojosa-Huerta, O.; Zamora, F.; Howard, K. Riparian vegetation dynamics and evapotranspiration in the riparian corridor in the delta of the Colorado River, Mexico. *J. Environ. Manage.* **2008**, *88*, 864–874. [CrossRef] [PubMed]
30. Nagler, P.L.; Murray, R.S.; Morino, K.; Osterberg, J.; Glenn, E.P. Scaling riparian and agricultural evapotranspiration in river irrigation districts based on potential evapotranspiration, ground measurements of actual evapotranspiration, and the Enhanced Vegetation Index from MODIS. I. Description of method. *Remote Sens.* **2009**, *1*, 1273–1297. [CrossRef]
31. Murray, R.S.; Nagler, P.L.; Morino, K.; Glenn, E.P. An empirical algorithm for estimating agricultural and riparian evapotranspiration using MODIS Enhanced Vegetation Index and ground measurements of ET. II. Application to the Lower Colorado River, U.S. *Remote Sens.* **2009**, *1*, 1125–1138. [CrossRef]
32. Nagler, P.L. Literature-Reviewed Estimates of Riparian Consumptive Water Use in the Drylands of Northeast Arizona, USA. In *U.S. Geological Survey Open-File Report 2020–1129*; U.S. Geological Survey: Flagstaff, AZ, USA, 2020; p. 9. [CrossRef]
33. AZMET. *The Arizona Meteorological Network*; University of Arizona: Tucson, AZ, USA; Available online: http://cals.arizona.edu/azmet/ (accessed on 12 December 2022).
34. Nagler, P.L.; Barreto-Muñoz, A.; Chavoshi Borujeni, S.; Jarchow, C.J.; Gómez-Sapiens, M.M.; Nouri, H.; Herrmann, S.M.; Didan, K. Ecohydrological responses to surface flow across borders: Two decades of changes in vegetation greenness and water use in the riparian corridor of the Colorado River delta. *Hydrol. Process.* **2020**, *34*, 4851–4883. [CrossRef]
35. Hunsaker, D.J.; Pinter, P.J.; Cai, H. Alfalfa basal crop coefficients for FAO–56 procedures in the desert regions of the southwestern US. *Trans. ASAE* **2002**, *45*, 1799–1815. [CrossRef]
36. Thornton, M.M.; Thornton, P.E.; Wei, Y.; Mayer, B.W.; Cook, R.B.; Vose, R.S. *Daymet: Monthly Climate Summaries on a 1-km Grid for North America, Version 4*; ORNL DAAC: Oak Ridge, TN, USA, 2020. [CrossRef]
37. Daymet: Daily Surface Weather and Climatological Summaries. Available online: https://daymet.ornl.gov/ (accessed on 25 July 2022).
38. Daly, C.; Taylor, G.H.; Gibson, W.P.; Parzybok, T.W.; Johnson, G.L.; Pasteris, P.A. High-quality spatial climate data sets for the United States and beyond. *Trans. ASAE* **2000**, *43*, 1957. [CrossRef]
39. Daly, C.; Halbleib, M.; Smith, J.I.; Gibson, W.P.; Doggett, M.K.; Taylor, G.H.; Curtis, J.; Pasteris, P.P. Physiographically sensitive mapping of climatological temperature and precipitation across the conterminous United States. *Int. J. Climatol. A J. R. Meteorol. Soc.* **2008**, *28*, 2031–2064. [CrossRef]
40. PRISM, Parameter-elevation Relationships on Independent Slopes Model. 2008. Available online: https://prism.oregonstate.edu/recent/ (accessed on 25 July 2022).
41. Colorado State University, Colorado Water Knowledge, Water Uses. Available online: https://waterknowledge.colostate.edu/water-management-administration/water-uses/ (accessed on 12 December 2022).
42. Maupin, M.A.; Ivahnenko, T.I.; Bruce, B. *Estimates of Water Use and Trends in the Colorado River Basin, Southwestern United States, 1985–2010*; SIR 2018–5049; U.S. Geological Survey: Flagstaff, AZ, USA, 2018. [CrossRef]
43. *PHSR, Hopi Preliminary Hydrographic Survey Report*; Arizona Department of Water Resources: Phoenix, AZ, USA, 2008.
44. Shirley, S.J.; Shelly, P.B. *The Navajo Nation Executive Branch*; Department of Dine Education, Navajo Nation: Window Rock, AZ, USA; Arizona Department of Water Resources: Phoenix, AZ, USA, 2010.
45. NRCE, Natural Resources Consulting Engineers. *Hopi Indian Reservation Riparian and Wetland Habitat Water Use Pasture Canyon*; U.S. Dept. of Justice, Environmental & Natural Resources Division: Denver, CO, USA, 2017.

46. USBR, U.S.; Bureau of Reclamation. Colorado River Basin Water Supply and Demand Study. 2012. Available online: https://www.usbr.gov/lc/region/programs/crbstudy/finalreport/Executive%20Summary/Executive_Summary_FINAL_Dec2012.pdf (accessed on 25 July 2022).
47. NAIP, National Agriculture Imagery Program, The USGS EROS Archive, Aerial Photography. Available online: https://www.usgs.gov/centers/eros/science/usgs-eros-archive-aerial-photography-national-agriculture-imagery-program-naip (accessed on 12 December 2022).
48. Jiang, Z.; Huete, A.; Didan, K.; Miura, T. Development of a two-band enhanced vegetation index without a blue band. *Remote Sens. Environ.* **2008**, *112*, 3833–3845. [CrossRef]
49. Huete, A.R.; Miura, T.; Kim, Y.; Didan, K.; Privette, J.P. Assessments of multisensor vegetation index dependencies with hyperspectral and tower flux data. In Proceedings of the SPIE 6298, Remote Sensing and Modeling of Ecosystems for Sustainability III, San Diego, CA, USA, 27 September 2006; Volume 6298, p. 629814. [CrossRef]
50. Didan, K.; Barreto-Muñoz, A.; Solano, R.; Huete, A. *MODIS Vegetation Index User's Guide (MOD13 Series) Vegetation Index and Phenology Lab*; The University of Arizona: Tucson, AZ, USA, 2015; pp. 1–38. Available online: https://vip.arizona.edu/MODIS_UsersGuide.php (accessed on 12 December 2022).
51. Allen, R.G.; Pereira, L.S.; Howell, T.A.; Jensen, M.E. Evapotranspiration information reporting: I. Factors governing measurement accuracy. *Agric. Water Manag.* **2011**, *98*, 899–920. [CrossRef]
52. Blaney, H.F.; Criddle, W.D. Determining water needs from climatological data. In *USDA Soil Conservation Service*; SOS–TP: USA, 1950; pp. 8–9.
53. FAO, United Nations Food and Agricultural Organization. Irrigation Water Management: Irrigation Water Needs, 1986, Chapter 3, Crop Water Needs. Available online: https://www.fao.org/3/s2022e/s2022e07.htm#3.1.3%20blaney%20criddle%20method (accessed on 12 December 2022).
54. NOAA, National Oceanic and Atmospheric Administration, NCEI, National Centers for Environmental Information. Available online: https://www.ncei.noaa.gov/ (accessed on 12 December 2022).
55. Nagler, P.L.; Glenn, E.P.; Nguyen, U.; Scott, R.L.; Doody, T. Estimating Riparian and Agricultural Actual Evapotranspiration by Reference Evapotranspiration and MODIS Enhanced Vegetation Index. *Remote Sens.* **2013**, *5*, 3849–3871. [CrossRef]
56. Huete, A.; Didan, K.; Miura, T.; Rodriguez, E.P.; Gao, X.; Ferreira, L.G. Overview of the radiometric and biophysical performance of the MODIS vegetation indices. *Rem. Sens. Environ.* **2002**, *83*, 195–213. [CrossRef]
57. Huete, A.R.; Glenn, E.P. Remote sensing of ecosystem structure and function. In *Advances in Environmental Remote Sensing*; Sensors, Algorithms, and Applications; CRC Press: Boca Raton, FL, USA, 2011; pp. 291–320.
58. Jarchow, C.J.; Nagler, P.L.; Glenn, E.P. Greenup and evapotranspiration following the Minute 319 pulse flow to Mexico: An analysis using Landsat 8 Normalized Difference Vegetation Index (NDVI) data. *Ecol. Eng.* **2017**, *106*, 776–783. [CrossRef]
59. Jarchow, C.J.; Nagler, P.L.; Glenn, E.P.; Ramírez-Hernández, J.; Rodríguez-Burgueno, J.E. Evapotranspiration by remote sensing: An analysis of the Colorado River Delta before and after the Minute 319 pulse flow to Mexico. *Ecol. Eng.* **2017**, *106*, 725–732. [CrossRef]
60. Jarchow, C.J.; Didan, K.; Barreto-Muñoz, A.; Nagler, P.L.; Glenn, E.P. Application and Comparison of the MODIS-Derived Enhanced Vegetation Index to VIIRS, Landsat 5 TM and Landsat 8 OLI Platforms: A Case Study in the Arid Colorado River Delta, Mexico. *Sensors* **2018**, *18*, 1546. [CrossRef] [PubMed]
61. Ponce-Campos, G.E.; Moran, M.S.; Huete, A.; Zhang, Y.; Bresloff, C.; Huxman, T.E.; Eamus, D.; Bosch, D.D.; Buda, A.R.; Gunter, S.A.; et al. Ecosystem resilience despite large-scale altered hydroclimatic conditions. *Nature* **2013**, *494*, 349–352. [CrossRef] [PubMed]
62. Nagler, P.L.; Barreto-Muñoz, A.; Sall, I.; Didan, K. Uncultivated Plant Water Use (Riparian Evapotranspiration) and Consumptive Use Data for Selected Areas of the Little Colorado River Watershed on the Navajo Nation, Arizona. U.S. Geological Survey Data Release; 2022. Available online: https://www.usgs.gov/data/uncultivated-plant-water-use-riparian-evapotranspiration-and-consumptive-use-data-selected (accessed on 12 December 2022).
63. Senay, G.B.; Friedrichs, M.; Morton, C.; Parrish, G.E.; Schauer, M.; Khand, K.; Kagone, S.; Boiko, O.; Huntington, J. Mapping actual evapotranspiration using Landsat for the conterminous United States: Google Earth Engine implementation and assessment of the SSEBop model. *Rem. Sens. Environ.* **2022**, *275*, 113011. [CrossRef]
64. Melton, F.S.; Huntington, J.; Grimm, R.; Herring, J.; Hall, M.; Rollison, D.; Erickson, T.; Allen, R.; Anderson, M.; Fisher, J.B.; et al. Openet: Filling a critical data gap in water management for the western united states. *JAWRA J. Am. Water Resour. Assoc.* **2021**, 1–24. [CrossRef]
65. Fisher, J.B.; Lee, B.; Purdy, A.J.; Halverson, G.H.; Dohlen, M.B.; Cawse-Nicholson, K.; Wang, A.; Anderson, R.G.; Aragon, B.; Arain, M.A.; et al. ECOSTRESS: NASA's next generation mission to measure evapotranspiration from the international space station. *Water Resour. Res.* **2020**, *56*, e2019WR026058. [CrossRef]
66. McVicar, T.; Vleeshouwer, J.; Van Niel, T.; Guerschman, J. Actual Evapotranspiration for Australia using CMRSET algorithm. Terrestrial Ecosystem Research Network. *Dataset* **2022**. [CrossRef]
67. Glenn, E.P.; Doody, T.M.; Guerschman, J.P.; Huete, A.R.; King, E.A.; Mcvicar, T.R.; Van Dijk, A.I.J.M.; Van Niel, T.G.; Yebra, M.; Zhang, Y. Actual evapotranspiration estimation by ground and remote sensing methods: The Australian experience. *Hydrological Processes* **2011**, *25*, 4103–4116. [CrossRef]

68. Guerschman, J.P.; Van Dijk, A.I.; Mattersdorf, G.; Beringer, J.; Hutley, L.B.; Leuning, R.; Pipunic, R.C.; Sherman, B.S. Scaling of potential evapotranspiration with MODIS data reproduces flux observations and catchment water balance observations across Australia. *J. Hydrol.* **2009**, *369*, 107–119. [CrossRef]
69. Abbasi, N.; Nouri, H.; Didan, K.; Barreto-Muñoz, A.; Chavoshi Borujeni, S.; Salemi, H.; Opp, C.; Siebert, S.; Nagler, P. Estimating Actual Evapotranspiration over Croplands Using Vegetation Index Methods and Dynamic Harvested Area. *Remote Sensing* **2021**, *13*, 5167. [CrossRef]
70. Hunsaker, D.J.; Fitzgerald, G.J.; French, A.N.; Clarke, T.R.; Ottman, M.J.; Pinter, P.J. Wheat irrigation management using multispectral crop coefficients. I. Crop evapotranspiration prediction. *Trans. ASAE* **2007**, *50*, 2017–2033. [CrossRef]
71. French, A.N.; Hunsaker, D.J.; Sanchez, C.A.; Saber, M.; Gonzalez, J.R.; Anderson, R. Satellite-based NDVI crop coefficients and evapotranspiration with eddy covariance validation for multiple durum wheat fields in the US Southwest. *Agric. Water Manag.* **2020**, *239*, 106266. [CrossRef]
72. Glenn, E.P.; Neale, C.M.U.; Hunsaker, D.J.; Nagler, P.L. Vegetation index-based crop coefficients to estimate evapotranspiration by remote sensing in agricultural and natural ecosystems. *Hydrol. Process.* **2011**, *25*, 4050–4062. [CrossRef]
73. Glenn, E.; Huete, A.; Nagler, P.L.; Nelson, S.G. Relationship between remotely-sensed vegetation indices, canopy attributes & plant physiological processes: What vegetation indices can and cannot tell us about the landscape. *Sensors* **2008**, *8*, 2136–2160.
74. Huete, A.R.; Didan, K.; van Leeuwen, W.; Miura, T.; Glenn, E.P. MODIS Vegetation Indices. In *Land Remote Sensing and Global Environmental Change*; Remote Sensing and Digital Image Processing; Ramachandran, B., Justice, C., Abrams, M., Eds.; Springer: New York, NY, USA, 2010; Volume 11. [CrossRef]
75. Glenn, E.P.; Nagler, P.L.; Huete, A.R. Vegetation index methods for estimating evapotranspiration by remote sensing. *Surv. Geophys.* **2010**, *31*, 531–555. [CrossRef]
76. Jarchow, C.J.; Waugh, W.J.; Didan, K.; Barreto-Muñoz, A.; Herrmann, S.; Nagler, P.L. Vegetation-groundwater dynamics at a former uranium mill site following invasion of a biocontrol agent: A time series analysis of Landsat normalized difference vegetation index data. *Hydrol. Process.* **2020**, *34*, 2739–2749. [CrossRef]
77. Jamison, L.R.; Johnson, M.J.; Bean, D.W.; van Riper, C. Phenology and Abundance of Northern Tamarisk Beetle, *Diorhabda carinulata* Affecting Defoliation of Tamarix. *Southwest. Entomol.* **2018**, *43*, 571–584. [CrossRef]
78. Nagler, P.L.; Nguyen, U.; Bateman, H.L.; Jarchow, C.J.; Glenn, E.P.; Waugh, W.J.; van Riper III, C. Northern tamarisk beetle (*Diorhabda carinulata*) and tamarisk (Tamarix spp.) interactions in the Colorado River basin. *Restor. Ecol.* **2018**, *26*, 348–359. [CrossRef]
79. McDaniel, K.C.; Bunting, D.P. Controlling Tamarisk Monocultures at the Bosque Del Apache National Wildlife Ref-uge: Lessons Along the Middle Rio Grande, New Mexico. In *Renewing Our Rivers: Stream Corridor Restoration in Dryland Regions*; University of Arizona Press: Tucson, AZ, USA, 2021; p. 244.
80. Nagler, P.L.; Sall, I.; Barreto-Muñoz, A.; Gómez-Sapiens, M.; Nouri, H.; Chavoshi Borujeni, S.; Didan, K. Effect of restoration on vegetation greenness and water use in relation to drought in the riparian woodlands of the Colorado River delta. *J. Am. Water Resour. Assoc.* **2022**, *58*, 746–784. [CrossRef]
81. Glenn, E.P.; Morino, K.; Didan, K.; Jordan, F.; Carroll, K.C.; Nagler, P.L.; Hultine, K.; Sheader, L.; Waugh, J. Scaling sap flux measurements of grazed and ungrazed shrub communities with fine and coarse-resolution remote sensing. *Ecohydrology* **2008**, *1*, 316–329. [CrossRef]
82. Bresloff, C.J.; Nguyen, U.; Glenn, E.P.; Waugh, W.J.; Nagler, P.L. Effects of grazing on leaf area index, fractional cover and evapotranspiration by a desert phreatophyte community at a former uranium mill site on the Colorado Plateau. *J. Environ. Manag.* **2013**, *114*, 92–104. [CrossRef] [PubMed]
83. Groeneveld, D.P.; Baugh, W.M.; Sanderson, J.S.; Cooper, D.J. Annual groundwater evapotranspiration mapped from single satellite scenes. *J. Hydrol.* **2007**, *344*, 146–156. [CrossRef]
84. Glenn, E.P.; Jarchow, C.J.; Waugh, W.J. Evapotranspiration dynamics and effects on groundwater recharge and discharge at an arid waste disposal site. *J. Arid. Environ.* **2016**, *133*, 1–9. [CrossRef]
85. Jarchow, C.J.; Waugh, W.J.; Nagler, P.L. Calibration of an evapotranspiration algorithm in a semiarid sagebrush steppe using a 3-ha lysimeter and Landsat normalized difference vegetation index data. *Ecohydrology* **2022**, *15*, e2413. [CrossRef]
86. Tabari, H.; Hosseinzadeh Talaee, P.; Some'e, B.S. Spatial modelling of reference evapotranspiration using adjusted Blaney-Criddle equation in an arid environment. *Hydrol. Sci. J.* **2013**, *58*, 408–420. [CrossRef]
87. Cleverly, J.R.; Dahm, C.N.; Thibault, J.R.; McDonnell, D.E.; Allred Coonrod, J.E. Riparian ecohydrology: Regulation of water flux from the ground to the atmosphere in the Middle Rio Grande, New Mexico. *Hydrol. Process. Int. J.* **2006**, *20*, 3207–3225. [CrossRef]
88. Tillman, F.D.; Callegary, J.B.; Nagler, P.L.; Glenn, E.P. A simple method for estimating basin-scale groundwater discharge by vegetation in the basin and range province of Arizona using remote sensing information and geographic information systems. *J. Arid. Environ.* **2012**, *82*, 44–52. [CrossRef]
89. Long, K.A. Integrating Satellite-Derived Precipitation Measurements to Assess Water Resources on the Navajo Nation and the Four Corners Region. Ph.D. Dissertation, University of Georgia, Athens, GA, USA, 2020. Available online: https://esploro.libs.uga.edu/esploro/outputs/doctoral/Integrating-Satellite-Derived-Precipitation-Measurements-to-Assess-Water-Resources-on-the-Navajo-Nation-and-the-Four-Corners-Region/9949365737402959 (accessed on 12 December 2022).

90. Nielsen-Gammon, J.W.; Fipps, G.; Caldwell, T.; McRoberts, D.B.; Conlee, D. *Feasibility Study for Development of Statewide Evapotranspiration Network*; Final report 1613581995; The Texas Water Development Board: Austin, TX, USA, 2017.
91. Caldwell, T.; Huntington, J.; Scanlon, B.; Joros, A.; Howard, T. *Improving Irrigation Water Use Estimates with Remote Sensing Technologies: A feasibility study for Texas*; Final Project Report; Agricultural Water Conservation Grants Texas Water Development Board: Austin, TX, USA, 2017.
92. Nagler, P.L.; Sall, I.; Barreto-Muñoz, A.; Didan, K.; Abbasi, N.; Nouri, H.; Schauer, M.; Senay, G.B. Evaluation of Two Types of Evapotranspiration Methods in Riparian Vegetation with the Two-Band Enhanced Vegetation Index and SSEBop in Restored and Unrestored Reaches of the Lower Colorado River in the USA. Available online: https://agu2022fallmeeting-agu.ipostersessions.com/default.aspx?s=F9-82-7F-A4-C7-D1-52-AA-CA-DF-37-BD-F5-B5-EF-88 (accessed on 12 December 2022).